Whole-Cell Voltage Clamp Recording

The voltage clamp is one of the most powerful techniques available for studying functional aspects of voltage-gated channels. Stepwise changes in voltage produced by this technique cause channels to interconvert between different states, and these transitions are monitored as changes in membrane current. The time course of this redistribution of states contains a great deal of information about the mechanism of channel gating. Furthermore, the voltage clamp can be used to activate different populations of channels selectively. In this way, a specific channel targeted by biological or pharmacological manipulations can often be identified and studied in detail. This protocol will focus on using the whole-cell voltage clamp to study voltage-gated channels, but it should be borne in mind that this technique is readily adapted to the study of ligand-gated channels, synaptic potentials, and exocytosis.

The voltage clamp measures current through a cell membrane while controlling the voltage. For the study of voltage-gated channels, voltage control has the obvious advantage of defining an important experimental condition that determines the functional state of a channel. Even with ligand-gated channels, which are nominally voltage independent, voltage dependence is often seen and electrical measurements are much easier to interpret if the voltage is held constant. Furthermore, for both voltage-gated and ligand-gated channels, the voltage sets the driving force for current through the membrane, so that when the voltage is fixed, the current reflects the number of open channels. In the absence of voltage control, the current flowing across the membrane changes the voltage by charging the membrane capacitance, and when this happens it is considerably more difficult to relate an electrical measurement to the functional state of a channel.

The whole-cell voltage clamp was an offshoot of the patch-clamp technique, which originally was designed for measuring current through single channels. In the early uses of the patch clamp, the voltage across a small patch of membrane on the surface of a cell was clamped by a glass micropipet with a tip of ~1 μm in diameter; hence the term patch electrode (Hamill et al., 1981). Subsequently, it was found that the patch of membrane under the electrode tip could be removed, and once this happened the electrode attained direct electrical contact with the cell interior. As a result, the voltage across the entire cell membrane was clamped instead of the voltage across the tiny patch (Fig. 6.6.1). This is how the technique came to be known as the **whole-cell voltage** or **patch clamp**. Because the technique depends on the ability to form a tight seal between the electrode tip and the plasma membrane of a cell targeted for study, it is also often called the tight-seal voltage clamp. These seals have an electrical resistance in the range of gigaohms (10^9 Ω), and are therefore known as "gigaseals." In the whole-cell voltage clamp, the patch electrode interior is in direct contact with the cell interior, providing a means of experimentally controlling the intracellular milieu (Fig. 6.6.1). This extends the utility of this technique considerably.

Other methods for voltage clamping cells had been devised prior to the development of the whole-cell method. These methods, which will not be discussed here, include the classical two-electrode voltage clamp, the intermittent or switching single-electrode voltage clamp, and the sucrose gap. They are generally applied to large cells, whereas the whole-cell voltage clamp performs better on relatively small cells (see Strategic Planning, discussion of the preparation). This is because any voltage clamp must perform two basic electrical functions: it must (1) control voltage and (2) measure current. The whole-cell voltage clamp uses a single electrode for both of these functions (Fig. 6.6.1), and because current flow creates a voltage drop across the electrode, large currents compromise

Contributed by Meyer B. Jackson

Current Protocols in Neuroscience (1997) 6.6.1-6.6.30

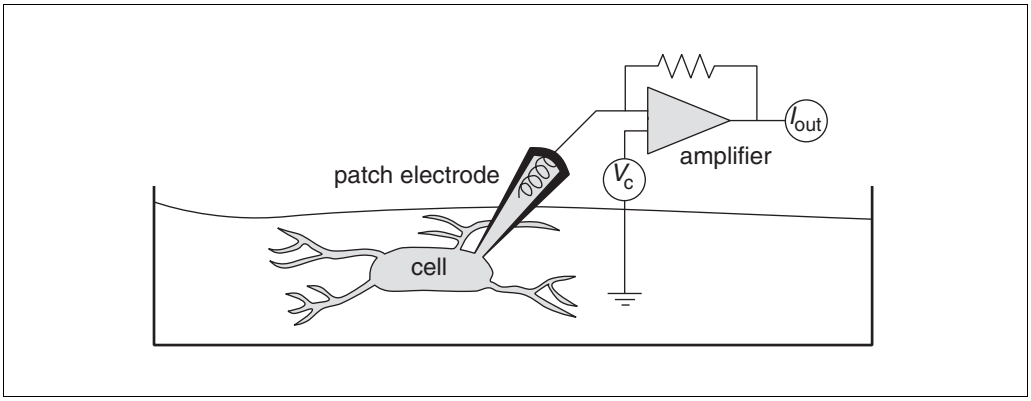

Figure 6.6.1 A sketch of a cell under whole-cell voltage clamp. A single cell is shown with a patch electrode and amplifier. The bathing solution superfuses the preparation while the pipet filling solution perfuses the cell interior. Because the patch-clamp amplifier circuitry maintains the same voltage at the two inputs, the command potential, V_c, will be applied to the cell. The amplifier output is a voltage proportional to the membrane current, and is designated I_{out}.

voltage control. Smaller cells generally have smaller membrane currents so that voltage control and current measurement with the same electrode is less of a problem. Despite the constraint of cell size, the whole-cell patch clamp is very versatile, and can be used in an extraordinarily diverse range of biological preparations.

The whole-cell patch clamp employs several other protocols from this chapter, including those dealing with various aspects of cell preparation (*UNITS 6.4 & 6.5*), instrumentation (*UNITS 6.1 & 6.2*), and electrode fabrication (*UNIT 6.3*). The method described here may also be useful in implementing other techniques, including capacitance measurement, patch clamp recording in brain slices, and analysis of synaptic potentials. The composition of solutions is an especially important consideration in voltage clamping the current through specific channels, and considerations relevant to different types of channels will be discussed. The mechanical steps of obtaining a whole-cell recording are enumerated: setting up the electrode and positioning it to make contact with the cell; obtaining a gigaseal; breaking in; making various electrical adjustments; taking actual measurements; and analyzing data. This is followed by a discussion of instrumental adjustments and refinements, as well as conceptual underpinnings.

STRATEGIC PLANNING

It is very important to optimize the patch clamp setup prior to experiments. The electronics should be tested on a model cell, the software installed and tested, the microscope optics adjusted, and the vibration isolation table tested for good isolation. Noise from the electronics should be minimized and 60-Hz line interference eliminated. The micromanipulator should be arranged to allow for easy electrode installation and positioning of the electrode tip within the full range of the field of view under the microscope. Cables should be connected between the amplifier, computer interface, and software; cables leading to the amplifier head stage and micromanipulators should be well secured to prevent vibrations. Time spent on these tasks will save a great deal of time later and greatly improve the success rate of experiments.

Electrophysiology Setup

As detailed in *UNIT 6.1*, a setup must be equipped with a microscope, oscilloscope, vibration isolation table, micromanipulator, and additional items as mentioned below. The microscope must be of sufficient quality to permit the user not only to see cells but also to make

out as much detail as possible on the cell surface, in order to locate regions where optimal contact can be realized between the electrode tip and the cell membrane. The micromanipulator must have sufficient resolution (<1 μm) to position the electrode tip accurately, and must have little drift (<1 μm), so that position does not change during recordings. In general, the demands on these visualization and positioning instruments are greater when cells are smaller or are located in brain slices.

Amplifier

Voltage is controlled and current measured with a patch clamp amplifier. Excellent patch clamp amplifiers are commercially available from Axon Instruments, Instrutech, and ALA Scientific Instruments (see *SUPPLIERS APPENDIX* for contact information on all suppliers mentioned in this unit). For whole-cell voltage-clamp experiments, an amplifier should have a low-noise current-to-voltage converter, and a capability for summation of holding potential and stimulus input. The amplifier should also have transient cancellation circuitry to provide a means of nulling the capacitative transient that accompanies any voltage change. Series resistance (R_s) compensation is a desirable feature when large currents are anticipated or when rapid settling times are needed. Additional parameters are discussed in *UNIT 6.2*.

Computer, Interface, and Software

A computer and computer interface have become standard parts of a voltage-clamp experiment. The computer uses an interface to acquire data through analog-to-digital converters and apply voltage command signals through digital-to-analog converters. Only a single channel of input (membrane current) and a single channel of output (command potential) are essential. The voltage monitor signal from a patch-clamp amplifier is not a true intracellular voltage reading and therefore has no more information about the cell than the voltage command signal from the computer. It can be viewed on an oscilloscope for various checking purposes, but it need not be saved as a separate channel of data. (This situation is quite different from the two-electrode voltage clamp, where the separate voltage electrode provides a true voltage measurement that can be used to evaluate the effectiveness of the clamp). The use of computers in patch clamping has become so standard that one commercially available patch-clamp amplifier, the EPC-9 (Instrutech or ALA Scientific Instruments), is under complete digital control. It has a built-in interface and cannot be used without a computer.

The computer, interface, and software replace several components of earlier voltage-clamp experiments, including the low-pass filter, pulse generator, and tape recorder. Although the computer system performs many of the functions previously left to an oscilloscope, it is still advisable to display signals on an oscilloscope for routine checking of the performance of the system. An inexpensive oscilloscope can perform this task.

A number of excellent software packages have been developed to run voltage-clamp experiments. These include the pClamp package (Axon Instruments) and Pulse (Instrutech). pClamp was originally developed for the PC; Pulse was originally developed for the Atari and now runs on Macintosh and PC. Axon Instruments and Instrutech also sell interfaces that allow the patch-clamp amplifier and other devices to be controlled by this software. An excellent program for voltage-clamp experiments with Macintosh computers has been developed as a PulseControl extension of the relatively inexpensive computer program IGOR (Wavemetrics). PulseControl can be down-loaded free of charge from the web site *http://chroma.med.miami.edu/cap* (Herrington and Bookman, 1994).

Electrode Holder

An electrode holder fitted with a silver chloride–coated silver wire connects the patch electrode to the amplifier head stage. This electrode holder must have a fitting to connect to a flexible plastic tube for the application of suction and pressure during certain steps in the experiment. Such electrode holders are available from the manufacturers of the patch clamp amplifiers mentioned above, as well as from E. W. Wright and World Precision Instruments. It is helpful but not necessary to have a pressure meter of some form to monitor and gauge the pressure. A particularly convenient system can be built with a digital voltage display and a pressure transducer from Sensym.

Patch Electrodes

Patch electrodes must be fabricated, coated, and fire-polished (see *UNIT 6.3*). Because dirt accumulates on the glass surface of the electrode and prevents sealing, electrodes should be used the same day. A key characteristic of an electrode is its resistance when filled with the patch-electrode filling solution. The resistance provides a useful indicator of the electrode tip size (*UNIT 6.3*; Sakmann and Neher, 1995a). Electrodes with resistances <1 MΩ are rarely used for whole-cell patch clamping because their tips are too large to obtain gigaseals reliably. With very small cells (<10 μm) it may be necessary to use small-tipped patch electrodes with resistances of ≥10 MΩ (Zhang et al., 1994). However, small-tipped, high-resistance electrodes generally lead to a higher R_s value, thus augmenting the R_s error (see Anticipated Results, section on point clamp effectiveness and R_s errors). To reduce resistances and keep tip sizes small, sharply tapered electrodes can be fabricated from thin-walled glass, although working with this kind of glass tends to be more difficult. To avoid the modifications of channel gating caused by ions released from soft glass (Cota and Armstrong, 1988), patch electrodes should be fabricated from hard glass.

Reducing electrode capacitance by applying a coating of low-dielectric material is very important. Without such a coating, the current transient that results from charging the electrode capacitance is large and difficult to separate from that which results from charging the cell. Without a clear separation of these two transients, cell capacitance and R_s cannot be measured and these key parameters of the recording will be indeterminate. Coating the electrodes can also lower the noise level to improve the signal-to-noise ratio, especially when recordings are made from small cells (<10 μm). This noise reduction often makes it possible to see single-channel steps in the whole-cell current (Fenwick et al., 1982; Zhang et al., 1994).

The most popular coating for patch electrodes is Sylgard (184 silicone elastomer, Dow Corning). When this material is used, the fire-polishing step must be performed after coating to burn off residue at the electrode tip that can interfere with seal formation. Sylgard is generally recognized as having the best electrical properties for coating patch electrodes, but other materials with a low dielectric constant such as Q-dope (GC Electronics), dental wax, or boat varnish have also been used. For some of these coatings time must be allowed for drying. The coating material should be transparent so one can see whether air bubbles are lodged near the electrode tip after filling. The coating should be applied with the aid of a small glass or plastic tool under a dissecting microscope, and cured immediately with an electric heating wire. For whole-cell voltage clamping it is not critical to cover the glass near the tip because this region has a small area; coating to within 100 to 200 μm is adequate. The coating must be applied high enough up the barrel to prevent any water contact with the glass walls of the electrode. This is important because the capillary action of water at the glass surface can turn the entire electrode wall into a large capacitative surface. The layer of coating is usually about as thick as the glass where the coating is applied. Refer to *UNIT 6.3* for additional information on coating electrodes.

Preparation

A biological preparation of cells or slices must be selected (see Chapter 3 and *UNITS 6.4 & 6.5*). In making this selection, one must consider the accessibility of the cell surface and the size and morphology of the cells. The accessibility of the cell surface is of prime importance because the formation of a gigaseal requires direct contact between the electrode tip and the plasma membrane. Gigaseals are thought to result from a direct molecular interaction between these two surfaces. To obtain a gigaseal, cells must have naked surfaces to provide free access for the patch electrode tip. Special conditions, treatments, and manipulations may be necessary to expose the cell surface and facilitate gigaseal formation.

Cell size is a consideration because the high capacitance of a large cell makes the settling time longer (see Anticipated Results, section on equivalent circuit and clamp settling time). Larger cells also tend to have large currents, and large currents lead to greater R_s errors (see Anticipated Results, section on point clamp effectiveness and R_s errors). The ideal cell for whole-cell voltage clamping is therefore small, on the order of 10 to 20 μm in diameter. Cells smaller than 10 μm can be patch clamped, but as the cells get smaller they pose a greater challenge to the manual dexterity of the experimenter. Even small cells can have currents that are large enough to cause significant errors in voltage control, but these problems can often be dealt with effectively by using low-resistance patch electrodes and R_s compensation.

Cell morphology is a consideration because long processes and elaborate morphologies cause space-clamp errors (see Anticipated Results, section on space-clamp effectiveness and cable analysis). There are few remedies for these errors, so where possible, morphological simplicity is a major advantage. There is often an enormous trade-off between technical ease of measurement and physiological relevance.

Physiological Bathing Solution

A bathing solution is needed for constant superfusion over the preparation (Fig. 6.6.1). This solution may be used while experiments are in progress or in the initial stages of the experiment prior to switching to a solution designed to enhance a particular component of ionic current (see Experimental Solutions, below, and see Critical Parameters and Troubleshooting, section on current separation). Physiological bathing solutions appropriate for various preparations can be found in the relevant journal articles.

Experimental Solutions

The compositions of the bathing solution and pipet filling solution are very important in the whole-cell voltage clamp. In formulating solutions, one must consider the ease of seal formation, the health of the preparation, and the specific objectives of an experiment. Because small amounts of dirt and debris can prevent gigaseal formation, the patch-electrode filling solution should be filtered with a 0.22-μm filter. This solution perfuses the inside of the cell (Fig. 6.6.1), providing a major technical advantage in isolating specific ionic components of current (see Critical Parameters and Troubleshooting, section on current separation). For each type of current to be studied it is necessary to provide the appropriate permeant ion, and it may also be necessary to block currents through other channels. It is not possible to provide recipes of solutions for each type of current because the requirements vary so widely between different types of cells and channels. It is therefore important to consult references dealing with a particular current in the relevant preparation. For references to exemplary studies of different channel types, see Background Information; for guidelines for solution design, see Critical Parameters and Troubleshooting.

One important general objective in the design of a patch pipet solution is to mimic the intracellular milieu. A key consideration in this regard is Ca^{2+} content. Although it is generally recognized that the free Ca^{2+} concentration is low inside cells, there is no general rule for how to adjust Ca^{2+} in a patch pipet solution. EGTA is the most widely used Ca^{2+} buffer. It is common to add 10 mM EGTA and 1 mM $CaCl_2$, which give a calculated free Ca^{2+} concentration of ~25 nM at pH 7.2, based on the relevant stability constants. However, free Ca^{2+} depends on other components of the solution and is quite sensitive to the purity of the EGTA. The EGTA concentration need not be as high as 10 mM. Lowering EGTA to <1 mM is common; removing it entirely does not always make recordings impossible, but recordings with low EGTA are generally more difficult to obtain and less stable. Another chelator, BAPTA, binds Ca^{2+} much more rapidly than EGTA, and this compound is often used when especially tight control of intracellular Ca^{2+} is desired. Some researchers suspect that BAPTA is unstable, and that it causes an increase in R_s (Bean, 1992). For these reasons, BAPTA-containing solutions should be prepared with a fresh supply of BAPTA less than ~2 weeks prior to use. It is generally not possible to obtain whole-cell patch-clamp recordings with solutions containing added Ca^{2+} and no chelator. Patch pipet filling solutions are generally stored frozen in 1-ml aliquots.

As K^+ is the major monovalent cation of cytoplasm, K^+ salts should be used in the absence of a good reason to do otherwise. When K^+ is replaced, the choice is often Cs^+ or *N*-methylglucamine, although *N*-methylglucamine has been reported to alter the behavior of Ca^{2+} channels (Malécot et al., 1988). Cytoplasmic Cl^- concentration varies among cell types, and can range from 5 to 40 mM. Although Cl^- is often used as the major anion of patch-pipet filling solutions, it is considered more physiological to replace most of the Cl^- with an organic anion, such as gluconate, aspartate, MOPS, acetate, citrate, or methanesulfonate. F^- is sometimes used to replace Cl^- when the goal is to poison all metabolic processes within a cell and free channels from modulatory influences. In most experiments, the patch pipet solution is buffered at a pH between 7.1 and 7.3 (usually with 10 mM HEPES). However, the pH can be varied to address questions regarding intracellular pH and membrane function. Titration of the buffer during solution preparation should be done with an acid or base of one of the major ions of the solution (e.g., a CsCl solution should be titrated with CsOH).

The activity of many channels depends on the addition of 1 to 10 mM ATP (Mg^{2+} salt). Even with ATP, rundown of Ca^{2+} current is difficult to avoid (Kostyuk, 1988), and a number of reagents have been added to patch-pipet filling solutions to prevent this. An ATP-regenerating system consisting of creatine phosphate and creatine phosphokinase has been reported to reduce rundown of Ca^{2+} currents (Forscher and Oxford, 1985). To maintain membrane currents dependent on G-proteins, 100 to 300 μM GTP is commonly added. More exotic additives may be used to test a hypothesis for regulation of channel function by a protein or signaling molecule. In such experiments, the time required for diffusional exchange between the pipet solution and cell interior should be considered. Exchange is roughly exponential in time, with a time constant τ (in seconds) that can be approximated by the following expression (Pusch and Neher, 1988):

$$\tau = 0.042\, R_s M^{1/3} C_c$$

Equation 1

where M is the molecular weight in Daltons (Da) of the substance in question, R_s is in megaohms, and C_c is the cell capacitance in picofarads. For R_s = 5 MΩ and C_c = 20 pF, this expression suggests that a 1000-Da molecule will exchange with the cell interior in 42 sec. Such exchange times are typical for whole-cell voltage-clamp recordings.

PATCH-CLAMP TECHNIQUE SETUP

Prior to an experiment several patch electrodes are fabricated and coated. The cells or slices should be ready. The instruments and computer are turned on and the software loaded. This protocol describes the establishment of a whole-cell voltage clamp and the verification of its efficacy.

Materials

Cells or tissue slice (see Chapter 3; and *UNITS 6.4 & 6.5*)
Patch electrode buffer (dependent upon experimental design; see Strategic Planning; see Critical Parameters and Troubleshooting)
Bathing solution (dependent upon experimental design; see Strategic Planning; see Critical Parameters and Troubleshooting)
Coated patch electrodes (see Strategic Planning and *UNIT 6.3*)
Electrophysiology setup (see Strategic Planning and *UNITS 6.1 & 6.2*)

Set up and position electrode

1. Fire polish and fill a patch electrode with solution. Mount the electrode in the electrode holder, which has been plugged into the amplifier head stage.

   Filling is easier if the tip is dipped in the solution for a few seconds and then filled from the back by inserting a thin tube.

2. Apply gentle positive pressure to the patch electrode interior through a tube connected to the electrode holder. With the pressure on, immerse the electrode tip by passing it through the surface of the bathing solution.

   Applying pressure while moving the electrode tip through the aqueous surface is important because dirt tends to accumulate at the air-water interface, and if this dirt gets on the electrode tip it can prevent gigaseal formation.

3. As soon as the tip is immersed, calculate the patch electrode resistance by applying a test pulse (typically 5 to 10 msec at 10 mV), reading the current, and using Ohm's law to calculate the resistance (Fig. 6.6.2A).

   For example, a 5-nA current with a 10-mV test pulse yields an electrode resistance of 2 MΩ. A low gain setting of the amplifier (1 mV/pA) is used in this step because the test pulse current is large. Typical starting resistances range from 1 to 10 MΩ.

   The resistance of the patch electrode should be monitored regularly during electrode positioning; increases in resistance prior to contact with a cell means the electrode tip has clogged and will be less likely to form a gigaseal.

4. Null the junction potential at the tip of the electrode with the appropriate control on the patch clamp amplifier (labeled Vp-offset on the EPC-7 and manual junction null on the Axopatch-1C).

   The junction potential between the bathing solution and the patch electrode solution should be measured in a separate experiment and used to correct voltages during data analysis according to Neher (1992).

5. With the course control of the micromanipulator, bring the electrode tip into the field of view containing a cell targeted for study (typical time: 1 min).

Establish gigaseal formation

6. Use the fine control of the micromanipulator to gently touch the electrode tip against the cell surface, check that the resistance has increased, and release the positive pressure (Fig. 6.6.2B).

   Sometimes the resistance increase will be small or imperceptible. Usually a slight depression of the cell surface is visible as the tip is pressed against the cell.

7. Using resistance and appearance as cues for contact between the cell surface and patch electrode tip, apply gentle suction to the patch pipet interior. The resistance should climb to >1 GΩ to produce a gigaseal (typical time: several seconds to several minutes).

The large rise in resistance results in a virtual flattening of the DC part of the test pulse current (i.e., the current following the transient; Fig. 6.6.2C). With a high gain setting for the amplifier (50 to 100 mV/pA), the DC current response will no longer appear flat but will show a small current on the order of 1 pA; a 10-mV test pulse to a 10-GΩ seal will give a current of 1 pA. Formation of a gigaseal may occur gradually, but sudden increases

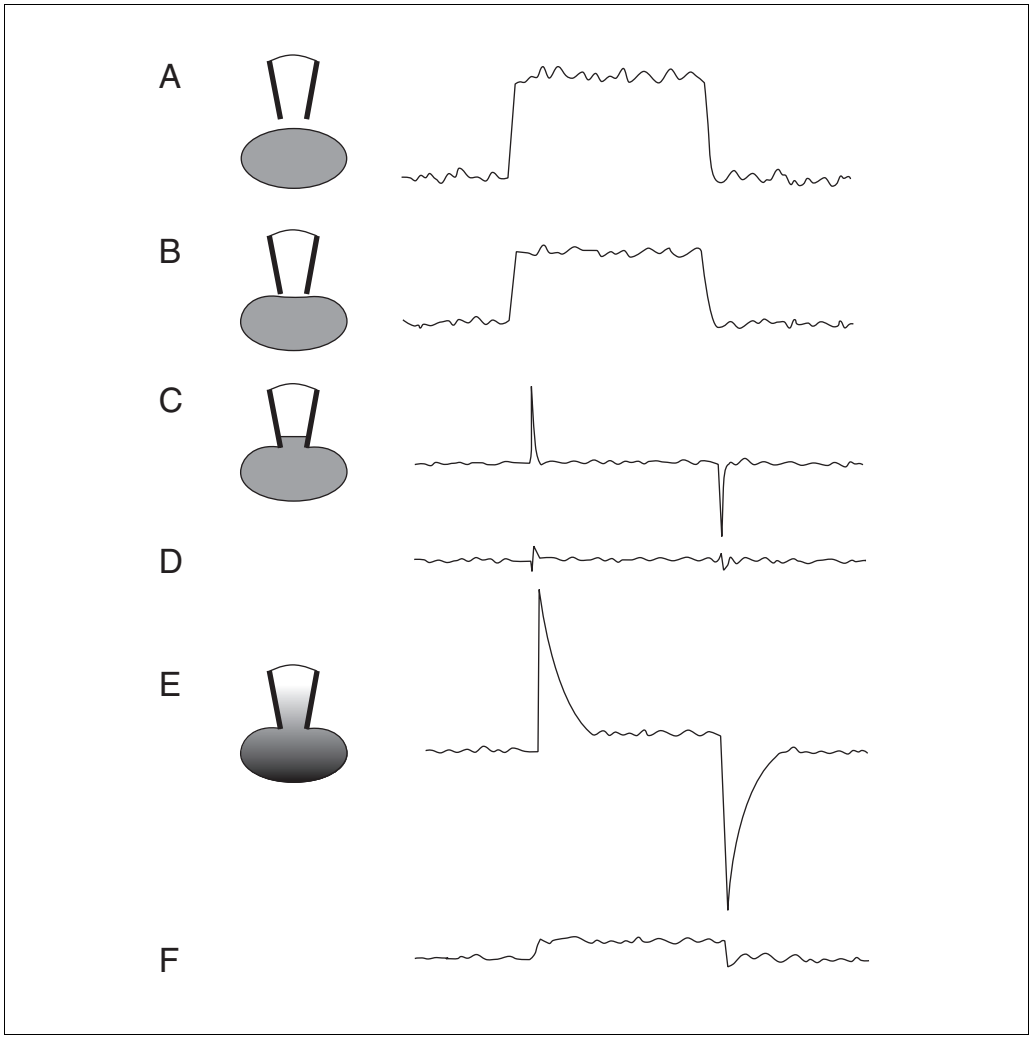

Figure 6.6.2 Test pulses produce different current responses as one proceeds through the establishment of a whole-cell voltage clamp recording. The physical relationship between the patch electrode and the cell is illustrated schematically on the left. The size of the current change produced by the test pulse goes down as the resistance across the patch electrode tip goes up. Thus, a reduction in test-pulse current indicates closer contact between the electrode tip and the cell. (**A**) The electrode is just above the cell, not in direct contact, so the resistance is low (1 to 10 MΩ) and the test pulse current is large. (**B**) The electrode touches the cell surface, the resistance goes up slightly, and the test pulse current gets smaller. (**C**) A gigaseal has formed as the result of gentle suction, which pulls a small patch of membrane up into the electrode tip. The resistance is high (>1 GΩ), so except for the transients, the test pulse current is virtually flat. (**D**) The electrode capacitance transient is nulled. (**E**) Break-in is achieved by strong suction that removes the patch of membrane in the electrode tip, but leaves the seal and cell intact. The resistance goes down and large capacitance transients are seen. Perfusion of the cell interior begins. (**F**) The whole-cell capacitance transient is nulled. Since steps D and F are purely electrical adjustments, the diagram of the cell and patch pipet is the same as in C and E, respectively.

in resistance are regarded as more auspicious. This step can be difficult; the suction strength necessary to achieve a gigaseal is highly variable. Seals with a resistance >5 GΩ are generally more likely to lead to a successful whole-cell recording. Sometimes a gigaseal simply fails to form even under optimal conditions. However, several failures in a row usually mean that there is a problem with some aspect of the preparation or solutions. For further discussion, see Critical Parameters and Troubleshooting, section on gigaseal formation.

Null the electrode transients

8. After achieving a gigaseal, verify that the test-pulse current is nearly flat except for transient spikes in opposite directions at the beginning and the end of the test pulse (Fig. 6.6.2C).

   These spikes reflect charging of the electrode capacitance, along with the much smaller capacitance of the membrane patch.

9. Null the transient by adjusting the appropriate patch-clamp amplifier controls to give a test-pulse response resembling that shown in Figure 6.6.2D. On an EPC-7, these controls are marked C-fast and τ-fast. The Axopatch 200 can null two electrode-charging transients with amplitude (MAG) and time constant (τ) controls (typical time: 15 to 30 sec).

   If these controls cannot be adjusted to null the electrode transients, then either the electrode has not been well coated with Sylgard or the solution level is high enough that the electrode glass above the coating has made contact with the bathing solution. As a result, the electrode capacitance is too high to be compensated with the amplifier circuitry. Although Sylgard coating very close to the electrode tip is not critical to reducing the electrode capacitance in whole-cell voltage clamping, the Sylgard should go as far back up the barrel of the electrode as the level of the bathing solution so that bare glass at the barrel does not touch water. If water touches the barrel it will rise up the outer walls by capillary action to form a thin film. This can add considerably to the electrode capacitance and defeat the purpose of the Sylgard coating. The height of the Sylgard coating needed on the barrel will vary depending on the angle at which the electrode is held and the depth of the bathing solution.

   It is important to maintain a constant depth of bathing solution during perfusion of the recording chamber, because changes in height will change the electrode capacitance (even with good Sylgard coating). It is common for perfusion systems to produce unsteady solution levels, and one can readily see the capacitance spikes wax and wane as the solution level rises and falls.

Perform break-in

10. Adjust the holding potential to the anticipated resting potential of the cell to avoid a large change in membrane potential upon break-in. Rupture the membrane patch under the electrode top by applying suction while watching the test pulse current. Increase the suction gradually, and stop immediately upon observing a sudden appearance of large spikes at the beginning and the end of the test pulse (Fig. 6.6.2E; typical time: 15 sec to several minutes).

    The large spikes indicate that break-in has taken place, as the test pulse then charges the cell interior and not just the patch electrode walls. The resistance also decreases upon break-in, allowing more DC current to be seen in the test pulse (Fig. 6.6.2E and F). Like gigaseal formation, this step can be quite difficult, and the suction strength required for break-in can be highly variable. Generally, stronger suction is needed to break in than to obtain a gigaseal. It is very important to stop the suction as soon as break-in is successful, because continued strong suction destroys the cell. This requires a very quick reaction. It is important that the test pulse be applied at a repetition rate >5/sec in order to see when break-in has occurred and react quickly. Sometimes break-in can be anticipated by subtle changes in the test pulse response, and these changes can be very helpful in permitting the experimenter to react quickly and stop suction. Recordings are often lost during this step.

Sometimes break-in occurs spontaneously, so steps 8 and 9 should be performed quickly, and the transient should be checked for changes prior to the application of strong suction.

Null the whole-cell transients

11. After break-in the test-pulse response reflects the passive charging of the cell. With the holding potential adjusted to a value of −80 to −100 mV (voltage-dependent channels are less active in this range), null the whole-cell charging transient by adjusting the appropriate amplifier controls, much as the electrode charging transient was nulled after gigaseal formation (typical time: 1 min).

    This adjustment eliminates the charging transient to give the test-pulse response, an appearance resembling Figure 6.6.2F. In recordings from cells with complex geometries only the fastest component of the whole-cell charging transient can be nulled. No effort should be made to remove the portion of the slower components associated with process charging, as this would lead to overcompensation of the cell body–charging transient and produce incorrect readings of R_s and cell-body capacitance (see Anticipated Results, section on space-clamp effectiveness and cable analysis).

    On the EPC-7 the controls are labeled C-slow and G-series. On the Axopatch 200 they are Whole Sell Capacitance and Series Resistance. The controls used to null the electrode transient often need not be touched during this step, but when the slow whole-cell adjustments fail to remove the transient completely it may be necessary to go back and forth between the fast and slow adjustments until the transient has been eliminated.

Note R_s and cell capacitance

12. Write down the cell capacitance, C_c, and R_s off the dials of the controls used to cancel the whole-cell transient. Calculate the clamp settling time, which is equal to R_sC_c (see Anticipated Results, section on equivalent circuit and clamp setting time). Calculate the cell resistance, R_c, from the amplitude of the test-pulse current using Ohm's law (Fig. 6.6.2F; typical time: 30 sec).

    Some computer programs can determine these parameters on line and save them automatically. The experimenter can also save a test pulse without canceling the transient to determine the parameters later during analysis off-line.

    Note that the G-series control on the EPC-7 actually gives the series conductance rather than resistance and this can be converted ($R = 1/G$; 1 μS gives 1 $M\Omega$). For cells with complex geometries the capacitance is that of the cell body, not that of the cell body plus a portion of the cell's processes (Jackson, 1992).

    C_c indicates the size of the cell or cell body. These numbers should always be noted down, as they are important parameters of the recording (see Anticipated Results, section on equivalent circuit and clamp setting time). The value of R_s is an extremely important indicator of the quality of the recording and of voltage control. It is generally advisable to choose a minimum acceptable value for R_s and discard recordings with higher values. Thus, the experiment often stops at this step and a new attempt must be initiated with another cell. The decision to discard should actually not be made until after attempting R_s compensation (step 13), as this may bring R_s into an acceptable range. The maximum acceptable R_s will vary depending on many factors. The discussions of the equivalent circuit and R_s errors (see Anticipated Results) provide some guidelines for setting a cutoff that is realistic and suitable for the goals of a particular study. Cutoffs can be <5 $M\Omega$ when large fast currents are being measured, or as high as 15 $M\Omega$ when the demands are less stringent. It is rare that a recording with an R_s >20 $M\Omega$ can be used for much in the study of voltage-gated channels. R_c also reflects the quality of a recording, with low values indicating leaky and often unhealthy cells. Thus, a minimum acceptable R_c can also be stipulated as appropriate for the cell type and experimental goals.

    C_c, R_s, and R_c can change during the course of a recording, so they should be checked periodically. Because C_c reflects membrane area, it can go up or down as a result of membrane trafficking in either direction, or because of excess hydrostatic pressure in the patch electrode. Drifts in whole-cell current are often accompanied by drifts in C_c,

indicating that the membrane that is gained or lost contains channels of interest. R_s tends only to go up, and this is thought to be due to physical obstruction of the patch electrode tip by cellular material. R_c goes down when the health of the cell deteriorates. The time that R_s and R_c remain below and above their respective cutoffs will determine how long the recording provides useful data.

13. *Apply R_s compensation (optional):* Slowly adjust the R_s compensation knob to increase the percent compensation while watching the test-pulse response. Record the R_s compensation setting for later correction of the R_s value noted in step 12 (typical time: 15 to 30 sec).

    As in step 10, a high repetition rate (5/sec) for the test pulse is helpful.

    R_s compensation is provided by most patch-clamp amplifiers. Because it is equivalent to reducing R_s, this feature can be very helpful in improving the time response and reducing R_s errors associated with large currents.

    R_s compensation is applied through controls on the patch-clamp amplifier that allow one to adjust the percent compensation and select a time-scale range. As R_s compensation is increased the small residual charging transients will get faster and larger and the noise will increase. A ringing of the charging transient will then appear and further increases in R_s compensation past a critical instability threshold will produce large rapid oscillations that are detrimental to the cell. Oscillations should be avoided, and the R_s compensation should be reduced immediately if oscillations start.

    The amount of R_s compensation that can be applied without causing oscillations varies greatly depending on the specific values of the circuit elements (Sigworth, 1995). A typical level of compensation might be 67%, and this would reduce the effective R_s by a factor of three.

    If R_s compensation is left very near the critical threshold for oscillation, small changes in R_s or C_c (step 12, final annotation) could cause the critical threshold for oscillations to be reached. When this happens the voltage will start to oscillate without warning and the cell will be destroyed. Therefore, a 10% to 20% safety margin should be allowed between the level of R_s compensation and the instability threshold.

14. Proceed to data acquisition and measurement of pulse sequences (see Basic Protocol 2).

DATA ACQUISITION AND PULSE SEQUENCES

BASIC PROTOCOL 2

Following the establishment of the whole-cell voltage clamp (see Basic Protocol 1), measurements can begin. In the study of voltage-gated channels, experiments usually involve application of some form of voltage step, generally in a carefully planned sequence. These pulses are almost always applied by a computer through an analog output connected to the stimulus input of the amplifier. The software packages presently available for voltage-clamp applications provide convenient user interfaces for designing pulse protocols. The software is also used to specify the digitization frequency for data acquisition and the bandwidth of a digital filter. The inverse of the filter corner frequency should be shorter than the time for the fastest channel gating transitions of interest, and the sampling frequency should be two or more times faster than the filter frequency. There is no point in filtering or sampling much faster than the time constant determined by R_sC_c, because the clamp is incapable of following more rapid processes (see Anticipated Results, section on equivalent circuit and clamp setting time). For further discussion of data acquisition, see Heinemann (1995).

Pulse Sequences

In most experiments, the holding potential and voltage of the test pulse are selected to change the channels from a closed state to an open one. The specific sequence of pulses will depend entirely on the question at hand. Examples of standard pulse sequences are

shown in Figure 6.6.3. To study the voltage dependence of channel activation, a series of steps are applied from a negative holding potential to a series of progressively more positive voltages producing progressively greater activation. Steps should be of sufficient duration to allow current to reach a desired endpoint, and are typically separated by intervals of 10 mV (Fig. 6.6.3A). To study the voltage dependence of inactivation, the holding potential prior to a depolarizing pulse is varied (Fig. 6.6.3B). This is often referred to as an h-infinity sequence because it determines the level of inactivation after equilibrium has been reached (from the h-infinity parameter of Hodgkin and Huxley, 1952b). If a channel is inactivated at positive voltages, then each step to an increasingly positive potential will be followed by less current activation during the subsequent test pulse to 30 mV (Fig. 6.6.3B).

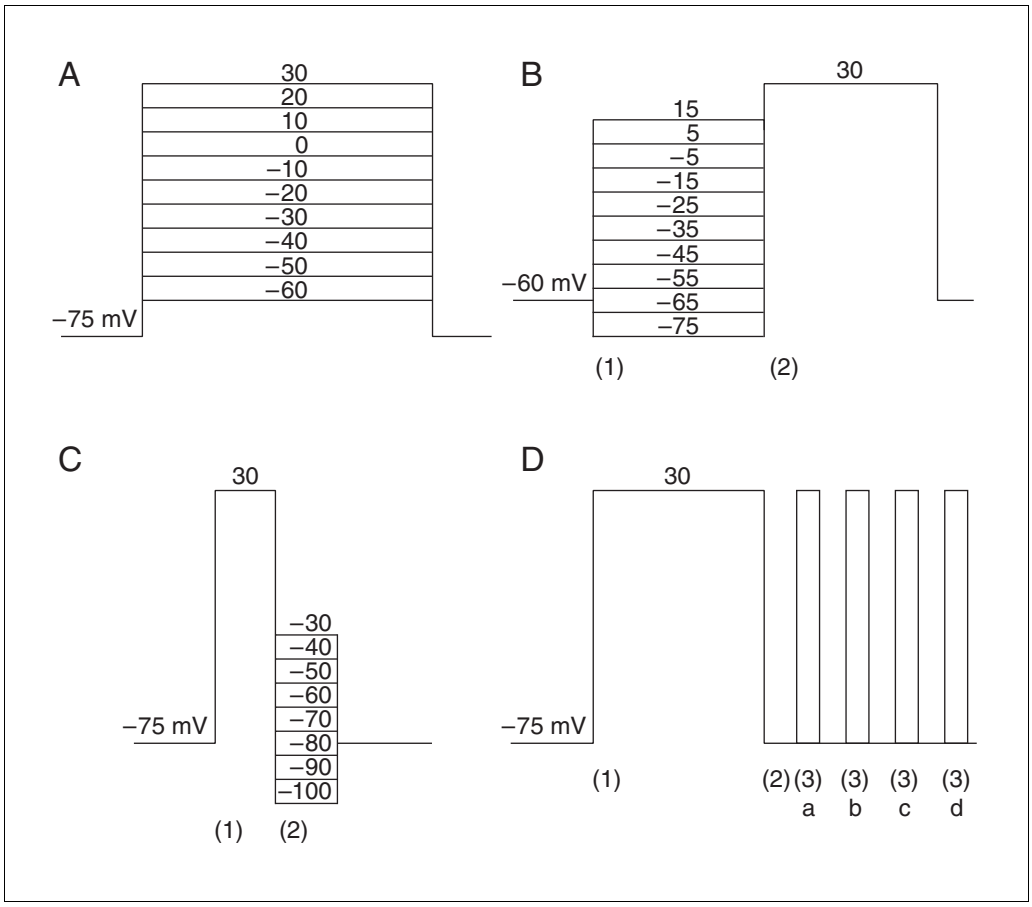

Figure 6.6.3 Pulse sequences for voltage-clamp experiments. Sequences such as these can be designed with software commonly used for whole-cell voltage clamping. (**A**) One of the simplest pulse sequences is a series of steps from the holding potential (–75 mV in this case) to –60, –50, …, and 30 mV. More positive voltage steps generally open more channels, but the voltage range where this occurs will vary depending on the type of channel under study. (**B**) A sequence of prepulses (1) varies the potential prior to a step to 30 mV. The step to 30 mV (2) activates channels that were not inactivated during the preceding pulse. Thus, the current evoked by the 30-mV pulse provides an assay for the extent of inactivation during the prepulse. (**C**) The voltage is varied after a 30-mV pulse to study the voltage dependence of tail currents. The pulse to 30 mV (1) activates the channels. The closing process can then by followed during the subsequent step to voltages ranging from –100 to –30 mV (2). For a K^+ channel with E_k = –80 mV, this sequence would move the voltage through E_k and reverse the tail currents. (**D**) Pulses presented in pairs separated by different time intervals are designed to study the kinetics of recovery from inactivation. Four pairs of pulses are indicated. The first pulse of the pair to 30 mV (1) is the same each time and inactivates most of the channels. The voltage is then returned to –75 mV (2) for variable amounts of time to allow variable amounts of recovery. Subsequent pulses to 30 mV (3a-3d) elicit currents that reflect the amount of recovery that has occurred in the intervening interval.

Figure 6.6.3C shows a pulse sequence designed to investigate how tail currents vary with voltage. After a positive test pulse to activate current, returning to a negative potential will close the channels. The decaying current after such a pulse is called a tail current. Reversal potentials of tail currents can be determined with a sequence like that in Figure 6.6.3C, and the reversal potential will be that of the channels that are open at the end of the immediately preceding voltage step. Thus, tail-current reversal potentials can be used to characterize the ion selectivity of the channel under study. Tail currents are also very useful in studying the kinetics of channel closure or deactivation.

In some voltage-clamp experiments the voltage is varied linearly rather than stepwise, to produce a voltage ramp. For noninactivating or slowly inactivating channels this method has the advantage of rapidly providing an indication of the voltage range in which a channel activates.

To study the kinetics of recovery from inactivation, the interval between the first inactivating pulse and the second test pulse can be varied (see Fig. 6.6.2D). To study the voltage dependence of recovery from inactivation one would use a similar sequence but with different voltages applied during the recovery interval.

The literature contains many inspiring examples of ingenious pulse protocols, some of which can be found in the references provided in Background Information. For example, one can hold the voltage positive to inactivate channels, then briefly jump to a negative voltage to produce a controlled amount of recovery from inactivation, and finally return to a positive voltage to reactivate channels and produce a current that reflects the distribution of channels initially in closed conformations lying along the pathway from the inactivated to the closed states (Oxford, 1981). The pulse sequence is generally the heart of a study of voltage-gated channels, and it is sound practice to attend carefully its design before starting an experiment. Designing a pulse sequence is often a creative process that can lead to the resolution of current through closely related channels and to the discovery of novel channel properties.

Leak Subtraction

Currents measured during a voltage-clamp experiment are a sum of channel current and leak current. Every membrane passes some current by leakage through voltage- and time-independent pathways. This current may reflect ion permeation through lipid bilayers or through poorly defined pathways involving unspecified membrane proteins. Leak current can be determined with voltage pulses applied in a range where the voltage-dependent channels are closed. The leak pulse sequence should be applied shortly before the experimental pulse sequence to avoid the problems from a slow change in membrane properties.

Leak subtraction is based on the assumption that leak current is linear so that it can be scaled to match the voltage change used to gate channels, and then subtracted from the current activated by a test pulse. This results in what may be considered a more pure channel current. Quite often the leak pulses are applied at a more negative voltage, say −120 to −140 mV. The design of a leak subtraction protocol is best made after examining the voltage dependence of membrane conductances in the cell under study to locate a window of voltage where nothing happens, i.e., where the voltage-gated channels remain closed. This will insure that the leak pulses do in fact measure leak current and not voltage-gated channel current. The amplitudes of the leak pulses are a small fraction, say 20%, of the amplitudes of pulses used to gate channels. Because leak current is often small, it is common to average several leak pulses. One of the most common leak subtraction protocols is called the P/4 procedure, where current evoked by four successive

pulses at one-fourth the amplitude of a test pulse are added together and then subtracted from the test-pulse response. P/*N* more generally refers to a procedure where the test pulses are divided by an integer *N* and applied *N* times to determine the leak current. Because leak subtraction is a common correction in voltage clamping, some commercially available voltage clamp software (e.g., Pulse from Instrutech or ALA Scientific Instruments and pClamp from Axon Instruments) includes an easily implemented leak subtraction feature, which can be performed on-line.

In addition to providing a more accurate measure of channel current, leak subtraction also produces a cosmetic improvement in the appearance of current traces by removing unsightly capacitance artifacts that remain despite adjustment of the transient cancellation circuitry of the patch-clamp amplifier (step 9). However, the smooth appearance of the current onset after leak subtraction must be viewed with caution. In such cases the current onset may simply reflect the clamp settling time, and therefore will provide little information about channel activation kinetics (Jones, 1990).

BASIC PROTOCOL 3

ANALYSIS OF PATCH CLAMP DATA

Analysis is an essential part of a voltage clamp study, and the computer programs used for controlling a voltage-clamp experiment have considerable analysis capability, or come with a separate analysis program.

Standard Analysis

The most common first step of analysis is plotting current versus voltage (perhaps from data obtained with a pulse sequence of the form in Fig. 6.6.3A). These current-voltage (I-V) plots generally reveal the voltage range that activates the channel. Further, when the I-V plot exhibits a reversal potential, the permeant ion can also be identified. Thus, such a plot provides an indication of the success of a current separation strategy (see Critical Parameters and Troubleshooting). Although I-V plots come in a bewildering variety of forms and shapes, the confusion is reduced considerably when one realizes that these plots are usually a product of two very simple functions, single-channel current and channel open probability (see Anticipated Results, section on current-voltage plots). Interpretation of an I-V plot in terms of these basic membrane properties is an essential first step in establishing the basic properties of a channel under study.

Once the permeant ion is known, the current can be divided by the driving force (the voltage minus the reversal potential) to give the conductance, which is directly related to the fraction of channels that are open. A plot of conductance versus voltage provides a direct view of the voltage-induced gating of the channel. These plots are generally interpreted in terms of specific models. The Boltzmann equation derives from a simple model for voltage gating based on the assumption that a channel undergoes a voltage-dependent transition between two states (see Anticipated Results, section on the Boltzmann equation). Current can also be fitted to the Boltzmann equation in the analysis of steady-state inactivation using a pulse sequence such as that shown in Figure 6.6.3B. Here the driving force is the same for each pulse, so changes in current will reflect changes in conductance.

In kinetic studies of membrane current, voltage-clamp data is analyzed by fitting a plot of current versus time to one or more exponentials. These fits generally yield time constants for the underlying kinetic processes (see Anticipated Results, section on exponential relaxations in channels). Quite often current through different types of channels can be resolved as distinct exponential components of current in a complex multiexponential process. It was found by Hodgkin and Huxley (1952b) that currents

activate with sigmoidal kinetics. Nearly all voltage-gated channels exhibit similar behavior, with a time course that is best represented by an exponential raised to an integral power (see Anticipated Results, section on exponential relaxations in channels). The exponents that characterize this sigmoidicity are also regarded as important parameters reflecting the molecular properties of the channel under study. For further discussion of analysis, see Heinemann (1995).

Cable Analysis (optional)

In cells with processes, cable analysis can be useful either in the characterization of cell morphology or in the evaluation of space-clamp efficacy (see Anticipated Results). The procedure for cable analysis described here is based on the assumption that the processes of the cell behave as a single cylinder with a sealed distal end and an electrotonic length equal to *L*. A current response is recorded to a 5 to 10 mV test pulse of 20 msec in duration. Because the slow components of the transient (which contain the most information about the process) are small in amplitude, it is generally advisable to average responses to as many as 50 pulses to reduce noise. The pulses can be applied at short intervals so that the entire recording can be completed in <10 sec. The software should make it possible to perform the averaging on-line. The test pulses should be applied in a voltage range where voltage-dependent currents are not active (typically more negative than –80 mV). To check that the response is purely passive, the decays at the onset and the end of the pulse should be compared. The averaged current is then fitted to a sum of as many exponentials as necessary (usually three or four, not including the rapid cell body–charging component balanced out in step 5). *L* and τ_m (the membrane time constant) can then be calculated from the slowest time constant, τ_1, and second slowest time constant, τ_2, with the following formulae.

$$L = \frac{\pi}{2}\sqrt{\frac{9 - \frac{\tau_1}{\tau_2}}{\frac{\tau_1}{\tau_2} - 1}}$$

Equation 2

$$\tau_m = \tau_1\left(1 + \left[\frac{3\pi}{2L}\right]^2\right)$$

Equation 3

The uses and interpretations of these parameters are discussed below (see Anticipated Results, section on space-clamp effectiveness and cable analysis), along with tests for the validity of the equivalent cylinder representation.

COMMENTARY

Background Information

Investigators have been using the voltage clamp for nearly 50 years (Cole, 1949; Marmont, 1949), during which an immense wealth of literature has developed. It is important to consult research articles for further experimental details on voltage-clamp techniques appropriate for specific channel and cell types. The classical papers in this field have great instructional value. The seminal work of Hodgkin and Huxley (1952a,b) in the squid axon employed a two-electrode configuration, and this work provides an excellent example of how the voltage clamp separates currents through different channels and quantifies underlying kinetic processes. Reports by Hamill et al. (1981) and Fenwick et al. (1982) served as the original expositions of whole-cell voltage-clamp methodology, and these works remain definitive. Excellent later discussions of voltage-clamp

methodology can be found in Smith et al. (1985), Jones (1990), and Sakmann and Neher (1995b).

Study of exemplary applications to specific types of channels is also recommended. The whole-cell voltage clamp has been used to study Na^+ channels in chromaffin cells (Fenwick et al., 1982), bull-frog sympathetic neurons (Jones, 1987), dorsal root ganglion neurons (Carbone and Lux, 1986), Schwann cells (Howe and Ritchie, 1992), and clonal pituitary cells (Cota and Armstrong, 1992). Representative studies of K^+ channels can be found for chromaffin cells (Marty and Neher, 1985), *Drosophila* muscle (Zagotta and Aldrich, 1990), GH3 cells (Oxford and Wagoner, 1989), peptidergic nerve terminals (Bielefeldt et al., 1992), and neurons from hippocampus (Numann et al., 1987), piriform cortex (Banks et al., 1996), and nucleus basalis (Yamaguchi et al., 1990). Ca^{2+} channels have been studied in chromaffin cells (Fenwick et al., 1982; Hoshi et al., 1984), intermediate pituitary cells (Cota, 1986), and neurons from hippocampus (Kay and Wong, 1987), thalamic reticular nucleus (Huguenard and Prince, 1992), bull-frog sympathetic ganglion (Jones and Marks, 1989), and dorsal root ganglion (Forscher and Oxford, 1985; Carbone and Lux, 1987; Fox et al., 1987; Swandulla and Armstrong, 1988).

Critical Parameters and Troubleshooting

Gigaseal formation

Difficulty in forming a gigaseal can be caused by any of the following. (1) Poorly exposed cell membrane: connective tissue, basement membrane, or flat, poorly visible cells can obstruct contact between the electrode tip and the target cell. (2) Dirt on the tip of the patch electrode: this can result from using older electrodes or from a failure to maintain positive pressure while passing the patch electrode tip through the surface of the bathing solution. (3) Incompletely cured Sylgard: during electrode fabrication, Sylgard should be cured immediately after application and prior to fire polishing. (4) Dirt inside the patch electrode: this can come from unfiltered solutions, dirt on the inner walls of the glass used for electrode fabrication, or a soiled silver wire in the electrode holder.

Many investigators have found empirically that adjusting the holding potential to a negative voltage (e.g., −80 mV) makes sealing faster and improves the success rate. No one really knows why this works, but it is probably related to the surface potential of the membrane. This attests to the extremely close contact that must exist between the electrode tip and cell membrane in order to form a gigaseal.

Current separation

The voltage clamp is often used to study one type of channel among the many present in a given cell. When this is the case, some procedure must be developed for separating the current through the channel of interest from the currents through any other channels. Current separation strategies fall into several broad categories, as summarized below.

Ionic dependence. The easiest form of current separation is isolation on the basis of permeant ion. The general strategy is to provide the ion of interest and eliminate the unwanted ions; thus, the technical ability to manipulate the solutions on both sides of the membrane provides a significant advantage. When elimination of unwanted ions is not possible, a limited isolation can be achieved by pulsing the voltage to the reversal potential of an unwanted ion. The current seen under these conditions reflects current through the channels that reverse at other voltages. Of course, this method does not lend itself to the study of voltage dependence, but important issues can often be addressed by this approach. It is better to design a solution that gives effective separation at all voltages. The following general guidelines will help in designing and modifying solutions for specific experiments (see also Swandulla and Chow, 1992, for additional details).

Na^+ currents. The bathing solution must contain Na^+, although an Na^+ channel–permeant ion such as Li^+ or ammonium can also be used. For all but very positive voltages, this provides a conducting ion to carry current through Na^+ channels into cells. Although intracellular Na^+ is not necessary to record an inward Na^+ current, a patch-pipet filling solution with a physiological concentration of Na^+ (~10 mM) has the advantage of defining the Na^+ Nernst potential and thus setting the driving force.

It is usually important to block K^+ channels, and K^+ current can be greatly reduced by using Cs^+ as the major cation in the patch-pipet solution. Further inhibition of K^+ currents can be achieved by adding any of a wide variety of blockers, such as a mixture of tetraethylammonium and 4-aminopyridine, to both the bathing solution and the patch-electrode solution. As the objective is to eliminate K^+ current, selectivity for different K^+ channel types is irrelevant and broad-spectrum channel block-

ers are preferred. An adequate block can generally be achieved with 10 to 20 mM tetraethylammonium and 1 to 5 mM 4-aminopyridine. Na^+ currents activate very rapidly to produce an early component of inward current before many K^+ channels open. This provides a way of checking that the K^+ channel blockers have no gross effects on Na^+ channels. Blockade of Ca^{2+} current is often not necessary when studying Na^+ current because Ca^{2+} currents are usually small; however, Ca^{2+} current can be blocked when necessary by adding 100 to 200 μM Cd^{2+} to the bathing solution.

K^+ currents. K^+ should be the major cation in the patch-pipet solution. For all but very negative voltages, this provides a conducting ion to carry outward current through K^+ channels. Blockade of Na^+ channels is usually an easy matter thanks to the potent and selective Na^+ channel blocker tetrodotoxin. Many Na^+ channels are blocked by 100 nM tetrodotoxin, but blockade of so-called tetrodotoxin-resistant Na^+ channels may require 1 μM tetrodotoxin. As with Na^+ current, the small magnitude of Ca^{2+} current in most cells relative to K^+ current usually makes blockade of Ca^{2+} channels unnecessary, but Cd^{2+} can be added if needed.

Ca^{2+} currents. Because most cells have Ca^{2+} currents that are smaller than K^+ and Na^+ currents, it is very important to block these other channels. To illustrate why, consider that a cell may have a peak K^+ current of 5 nA and a peak Ca^{2+} current of 100 pA (e.g., at −10 mV). This means that a 99% block of K^+ current will still leave 50 pA of unblocked K^+ current. Since these currents are opposite in sign, the apparent Ca^{2+} current will appear to be only 50 pA, or half of the true Ca^{2+} current. Thus, minute amounts of unblocked K^+ current will produce large errors in Ca^{2+} current. Likewise, unblocked Na^+ current will produce artificially large measurements of Ca^{2+} current. Na^+ channels can be blocked with tetrodotoxin as mentioned above (see K^+ currents). Blockade of K^+ current is one of the greatest challenges to obtaining Ca^{2+} current recordings of high quality. The K^+ channel blocking procedures mentioned above (see Na^+ currents) also apply to the measurement of Ca^{2+} current. Cs^+ addition to the pipet solution reduces K^+ current substantially, but often not completely. Furthermore, Cs^+ weakly permeates Ca^{2+} channels to produce significant outward currents (Bean, 1992). These issues require special attention on a case-by-case basis.

Increasing the extracellular [Ca^{2+}] and substituting Ba^{2+} for Ca^{2+} are common measures for improving the quality of Ca^{2+} current recordings. When extracellular [Ca^{2+}] is increased, phosphate must be reduced or removed because of the low solubility of $Ca_3(PO_4)_2$. Ba^{2+} often permeates Ca^{2+} channels more easily than Ca^{2+} itself (thus producing a larger current). Ba^{2+} has the additional advantage of blocking K^+ channels, but if Ba^{2+} is used it must be borne in mind that Ba^{2+} usually alters Ca^{2+} channel properties such as voltage dependence and inactivation kinetics.

Other currents. Not every channel of interest is a Na^+, K^+, or Ca^{2+} channel. Channels gated by neurotransmitters are often broadly selective for cations or anions, and the solutions must be designed accordingly. The study of a channel with a novel ion-permeability profile will require the design of bathing and patch-electrode solutions that optimize current through that channel.

Verification. It is important to verify any strategy for separation of different ionic components of current. One of the most powerful arguments that can be made for successful separation is to check that a current reverses at the Nernst potential for the permeant ion. When possible, the Nernst potential should be altered by changing the intracellular and extracellular concentrations of the permeant ion to see that the reversal potential moves accordingly.

Voltage dependence

A plot of current or conductance versus voltage will quite often show two or more distinct components of current activation, reflecting a difference in the voltage dependence of different channel types. The voltage of a pulse can then be strategically selected to activate one type of channel or another. Channels inactivate at different voltages as well, so that the holding potential can be chosen to inactivate one type of channel but not another. In particular, T-type Ca^{2+} channels are well known for their requirement of a holding potential more negative than approximately −70 mV. Thus, a depolarizing pulse from a more positive holding potential will activate other types of Ca^{2+} channels, but not T-type. Likewise with K^+ channels, the A-current is inactivated at more positive potentials so that the holding potential can be adjusted to eliminate this current. A current eliminated by this strategy can also be isolated. Subtracting the current evoked by a pulse preceded by an inactivating holding potential from the current evoked by a pulse to the

same voltage preceded by a noninactivating holding potential yields the inactivating current.

Kinetics

Currents can also be resolved on the basis of kinetic properties. In the squid giant axon, the current seen 1 msec after a voltage step is almost entirely through Na^+ channels, whereas the current seen 10 msec later is almost entirely through K^+ channels (Hodgkin and Huxley, 1952b). The time course of current relaxation at a given voltage may have complex multiexponential kinetics, and sometimes current through different channels can be assigned to different exponential components. There are many such examples, not only in activation kinetics, but in tail-current decay and inactivation kinetics as well. However, because a channel can exhibit multiexponential kinetics, assigning different exponential components of current to different channel types is very risky without some form of corroborating evidence based on another separation strategy.

Pharmacology

Even when channels are remarkably similar in biophysical characteristics, they can be separated very cleanly if the right drug is available. The use of tetrodotoxin was mentioned earlier for eliminating Na^+ channels. In recent years a number of naturally occurring toxins have been isolated from the venoms of exotic creatures. Some of these toxins exhibit extraordinary selectivity for specific types of channels. In cases where high selectivity is achieved, these reagents can eliminate current through a single channel type so that subsequent subtraction from the control current provides an isolated current through the blocked channel. A recent compilation of neurotoxins by *Trends in Neurosciences* (Adams and Swanson, 1996) can be used as a reference in the selection of toxins with actions at specific types of ion channels. Catalogs from companies such as Alexis, Alomone Labs, Bachem Bioscience, Biomol, Calbiochem, LC Laboratories, and Research Biochemicals International provide up-to-date information on available toxins with references often included. New toxins continue to be discovered and characterized at a rapid pace. Using toxins and drugs to isolate current through different channel types can work well, but it is advisable to verify selectivity in the particular cell type under study. Any actions at other channels, including partial block or modification of properties, can produce very misleading results.

Intracellular manipulations

A current separation strategy can exploit different dependencies of channels on cytoplasmic factors. Current through Ca^{2+}-activated K^+ channels can often be eliminated by adding 10 mM BAPTA to the patch pipet filling solution. Current through channels that depend on intracellular ATP or GTP can be eliminated by omitting these substances. Knowledge of the detailed cellular and metabolic requirements of different channel types can be of great value in developing strategies along these lines.

Additional considerations

The various methods of current separation discussed above (based on ionic dependence, voltage dependence, kinetic behavior, drug sensitivity, and cellular requirements) can form a powerful combination in the isolation of current through a selected channel. However, the process of current separation has many pitfalls: drugs may lack specificity, and the voltage dependence and kinetic properties of channels can be exceedingly complex. Furthermore, it is not uncommon for a cell to have ten or more distinct types of ion channels. A cell may have five types of K^+ channels, and voltage-clamp techniques alone are unlikely to resolve all of them. In such situations it may simply not be possible to decide whether the results are more consistent with a certain number of channel types with simple properties or a smaller number of channel types with more complex behavior. In these situations combining the voltage clamp with other techniques may be necessary. Single-channel recording is especially useful in these situations because the single-channel current can be used as a defining property. A few single-channel recordings often provide a clear resolution of an issue in which voltage-clamp data alone is ambiguous. Sensitive molecular techniques such as single-cell PCR (Monyer and Jonas, 1995) and immunoblotting (see *CPMB UNIT 10.8* and *APPENDIX 1A* in this manual) may also help in determining which channel types are present in a particular cell.

Equivalent circuit and clamp settling time

To understand the passive electrical response of a clamped cell to a voltage change, consider the equivalent circuit shown in Figure 6.6.4. The cell is represented by a resistor and capacitor in parallel, represented by their resistance R_c and capacitance C_c, respectively. The

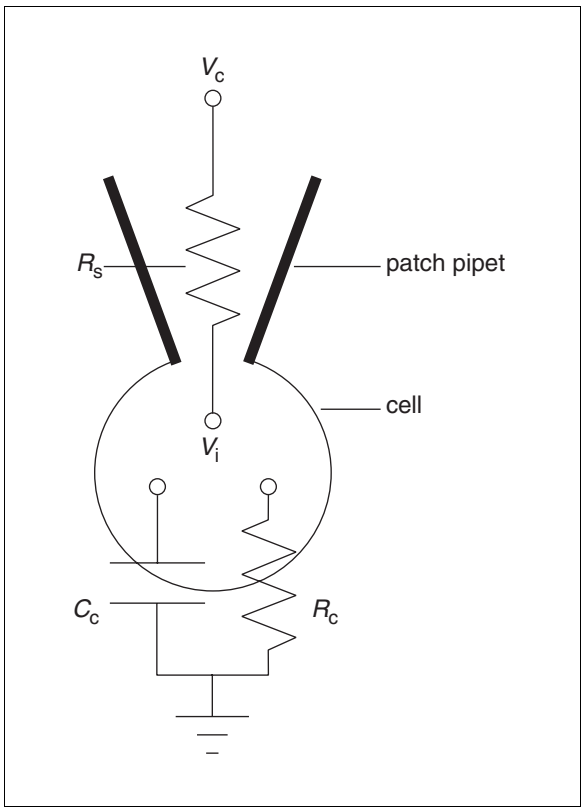

Figure 6.6.4 The equivalent circuit of a whole-cell voltage-clamp recording. A patch electrode is shown with access to the cell interior. The series resistance, R_s, is shown through the tip of the patch electrode connecting the patch-clamp amplifier command potential, V_c, with the potential inside the cell, V_i. The resistance and capacitance of the cell are represented by R_c and C_c, respectively.

patch electrode is represented by the series resistance (R_s), so-called because it is in series with the circuit elements representing the cell. (Because this resistance is also in the access pathway to the cell interior, it is sometimes referred to as access resistance.) When the command potential applied by the amplifier to this circuit is abruptly changed from zero to V_c, the current changes with the time course

$$I = V_c\left(\frac{1}{R_c + R_s} - \frac{1}{R_s}\right)(1 - e^{-t/\tau}) + \frac{V_c}{R_s}$$

Equation 4

where

$$\tau = \frac{C_c R_c R_s}{R_s + R_c} \approx R_s C_c$$

Equation 5

The approximation on the right side of Equation 5 is based on R_c being much larger than R_s. This time constant is a basic index of the speed of the clamp. Channel gating processes faster than this cannot be measured accurately without special approaches, such as R_s compensation (see discussion of point-clamp effectiveness and R_s errors). After the clamp settles, the voltage in the cell is related to the command voltage by the expression

$$V_i = \frac{V_c R_c}{(R_s + R_c)}$$

Equation 6

and again the condition that $R_c >> R_s$ is useful because it leads to the expression

$$V_i \approx V_c$$

Equation 7

Equation 6 makes the point that the circuit behaves as a simple voltage divider between R_c and R_s, and when $R_c >> R_s$, most of the voltage drop occurs across R_c to give Equation 7. Immediately after a voltage pulse, the current starts off at V_c/R_s, because before any current has flowed the voltage drop is entirely across the patch electrode R_s. The current then relaxes exponentially with a time constant of $\approx R_s C_c$ to a final value of $\approx V_c/R_c$. This relaxation can readily be seen in a whole-cell voltage-clamp recording by turning the whole-cell transient cancellation circuitry off while looking at the test-pulse response. The transient cancellation circuitry of the amplifier simply removes this

transient from the output signal, but the charging of the cell follows this time course regardless of whether the transient cancellation circuitry is on or off. In fact, the whole-cell voltage clamp provides no direct measure of V_i, but only sets V_c. This means that the experimenter must understand the relationship between these two voltages and be prepared to evaluate and correct discrepancies.

This analysis makes clear the advantages of a low R_s. A low R_s shortens the settling time to permit the study of faster channel-gating processes. Voltage errors after clamp settling are caused by large currents or low values of R_c, and these errors are also reduced. In summary, a low R_s improves both the speed and fidelity of the voltage clamp.

Point-clamp effectiveness and R_s errors

The preceding section made the point that the voltage in the cell, V_i, is approximately equal to the voltage applied to the patch electrode, V_c, as long as R_c is much greater than R_s. The effectiveness of the voltage clamp just beyond the tip of the patch electrode depends on the validity of the approximation $V_i \approx V_c$. This defines a basic index of performance of the voltage clamp, often referred to as point clamp. For any of a number of reasons the gap between R_s and R_c may fall, compromising the effectiveness of point clamp. For example, when channels in the cell membrane open, R_c can become small so that V_i will deviate from V_c even when R_s is very low. For a membrane current equal to I_m, Ohm's law gives the deviation as $I_m R_s$. For R_s = 10 MΩ, a 1-nA current produces a 10-mV R_s error. Larger values of both current and R_s are common and result in a larger error. The problem is compounded by the voltage dependence of the channels themselves. If the error changes the voltage in such a way as to make more channels open, the increase in inward current through the membrane will increase the error. This positive feedback can make the voltage dependence of channel activation appear to be much steeper than it actually is (Armstrong and Gilly, 1992; Marty and Neher, 1995). The opposite distortion is seen with outward currents. As channels open, the increasing error will move the voltage away from voltages which gate the channels, and this will make channel activation appear as a less steeply rising function of voltage. R_s also slows the settling time of the clamp (Equation 5) to make the kinetics of rapidly gated channels appear slower.

Two basic strategies are available for reduction of R_s errors. The first is to lower the resistance of the patch electrode, as R_s is approximately two- to three-fold higher than the electrode resistance prior to patching. Electrodes with large-diameter tips and wide tapers can be fabricated to obtain resistances on the order of 1 MΩ. Patch-pipet filling solutions with inorganic instead of organic ions (i.e., using Cl^- instead of gluconate) reduce both the initial patch-electrode resistance and R_s, because inorganic ions have higher mobilities.

The second strategy for reducing R_s error is an electronic procedure known as R_s compensation. This is implemented with a circuit that uses the current together with the setting of R_s adjusted by the experimenter, and electronically computes a correction that is added to the command potential. In this way a specified percentage of the R_s is corrected for (see Sigworth, 1995, for a discussion of R_s compensation). For all intents and purposes, the behavior of a compensated R_s is electrically indistinguishable from a lower R_s. The charging time and voltage in the cell are described by Equations 5 and 6, respectively, with the compensated value in place of the true value of R_s. Even with regard to cable properties (see discussion of cable analysis), the effect of R_s compensation is perfectly modeled by a reduction in the value of R_s.

Space-clamp effectiveness and cable analysis

The discussion in the preceding two sections on the dynamics and errors of the whole-cell voltage clamp was based on the simple equivalent circuit shown in Figure 6.6.4. This equivalent circuit is valid for cells with simple shapes, but neurons usually have extensive axonal and dendritic processes. Just as current flowing across the R_s of the patch electrode will cause the voltage at the tip of the electrode to deviate from the command voltage, current flowing across the cytoplasmic resistance inside a process will cause the voltage in distal parts of the cell to deviate from the voltage in the cell body. This can lead to large errors even when the point-clamp performance is perfect. If a process is very long, the voltage across the membrane in distant segments may be completely unaffected by the voltage clamp. In general, the membrane potential will deviate from the command potential to a degree that varies with the distance from the patch electrode.

This aspect of the performance of a voltage clamp is known as space clamp. Space-clamp errors have made it virtually impossible to use

the whole-cell voltage clamp to characterize Na^+ and Ca^{2+} currents in neurons in brain slices. As a result, the best studies of these channels in neurons have been undertaken in dissociated cells, where processes are relatively short, or in excised patches, where space clamp is not an issue. Poor space clamp is a more difficult problem to deal with than poor point clamp. Unlike R_s errors, most space-clamp errors cannot be reduced by better electronics or electrodes. Therefore, the discussion here will focus on evaluating the errors so that the experimenter will at least understand the limitations imposed by this problem.

One of the first clues that space clamp is poor is the appearance of characteristic artifacts in the recorded current. Because poor space clamp often coincides with good point clamp, one often sees well-clamped currents superimposed upon delayed currents which appear to have R_s errors. Even when well-clamped currents flow through the membrane of the cell body, distal portions of membrane under weak voltage control will often be depolarized enough to gate channels, and if these channels can produce inward current, the inward current will further depolarize the membrane to produce an action potential. This will be seen by the voltage-clamp amplifier as an inward current that follows the time course of an action potential. Even if the control of voltage is good enough to suppress an action potential, the tug-of-war between the channels and the voltage clamp for control of the voltage across distal portions of membrane will narrow the range of V_c over which channel activation is seen, and the resulting error will be similar to that produced by a high R_s. Because the voltage change takes more time to spread to distal processes, a poorly clamped inward current may appear well after the onset of the current through the well clamped membrane near the patch electrode. This superposition may produce conspicuous notches in a current record; however, if the error is less severe, a kinetic process will be temporally "smeared," making the problem more difficult to recognize.

Because K^+ channels do not produce action potentials, the problems with space clamp are less conspicuous and often less severe than they are for Na^+ and Ca^{2+} channels. K^+ channels at the spatial limits of the clamp tend to halt the spread of voltage so that poorly clamped membrane does not produce much current. Thus, K^+ currents recorded from neurons in brain slices often qualitatively resemble K^+ currents recorded from cells without processes. However, the resemblance may be deceptive. Poor space clamp can still distort the time course, particularly when channel gating is rapid, and this should be checked on a case-by-case basis. Furthermore, determination of the current density is more difficult because the area through which the measured current flows is unknown. Distortions can be checked by comparing whole-cell currents with channel current in cell-attached (Bielefeldt et al., 1992) or excised patches (Jackson and Zhang, 1995). Alternatively, quantitative representations of channel kinetics (Hodgkin and Huxley, 1952b) can be fed back into a computer model that simulates the behavior of a cell with a complex geometry. If the cell morphology is known either from cable analysis or cell labeling, then simulations of voltage-clamp experiments with different channel distributions can evaluate the possibility that poor space clamp distorts the data. A good computer program for performing such simulations is Nodus (De Schutter, 1989), and this method has been used to evaluate the effect of cell geometry on K^+ channel properties in cortical pyramidal cells (Banks et al., 1996).

To evaluate space-clamp errors quantitatively, one must abandon the equivalent circuit of Figure 6.6.4 and develop a model that reflects the geometrical complexity of the cell under study. Because neuronal processes often have a cable-like shape, the development of such models falls under the heading of cable theory. In contrast to the single exponential response of a simple cell (see section on the equivalent circuit and clamp setting time, above), in a geometrically complex cell the response to a voltage pulse is a sum of two or more exponentials. Some neurons, such as Purkinje cells, can be adequately represented by two compartments (rather than a cable), and the cell charging current is then a sum of two exponentials (Marty and Neher, 1995). The charging of both of these compartments is a function of R_s, so R_s compensation can reduce the time for charging the distal compartment in Purkinje cells. This is a rare case where the space-clamp error can be partially corrected instrumentally.

Unfortunately, the two-compartment case seen in Purkinje cells is exceptional; most neurons exhibit more complex electrotonic behavior. Dendrites often have extensive branches, and it was shown by Rall (1959) that under special conditions of branching, a dendritic arbor will exhibit passive electrical responses (electrotonic behavior) identical to that of a single equivalent cylinder. This has made the

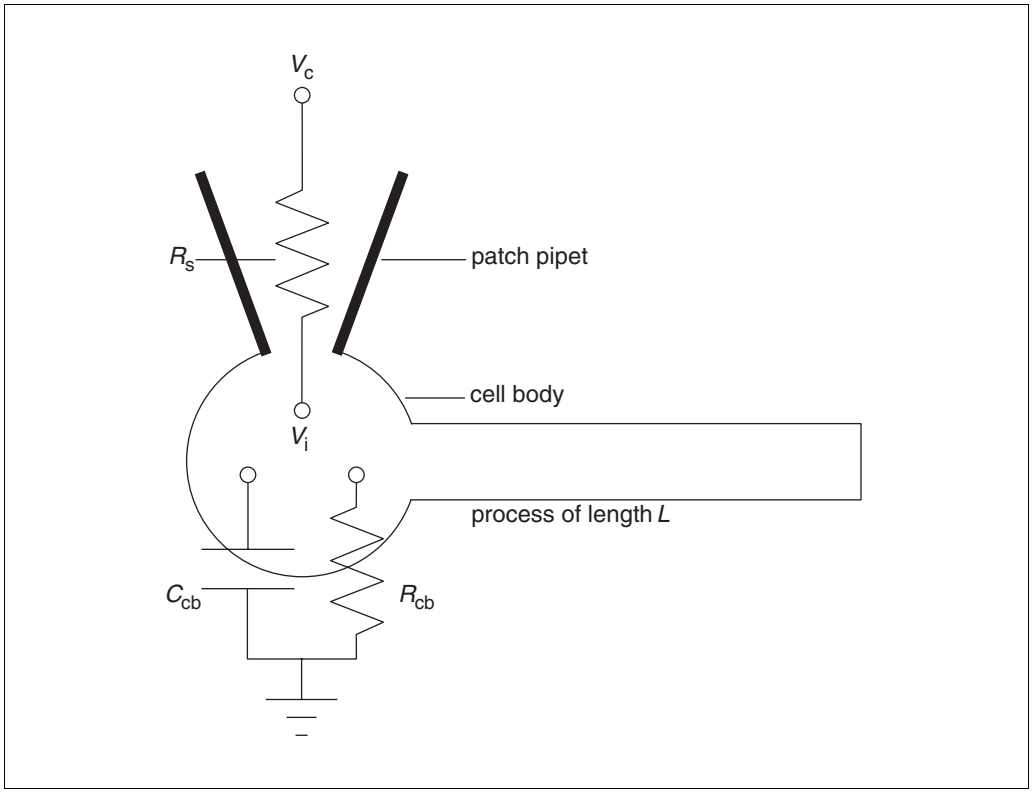

Figure 6.6.5 The equivalent circuit of a whole-cell voltage clamp recording from a cell with a cylindrical process. Symbols are as in Figure 6.6.4, except that the resistance and capacitance of the cell body are labeled R_{cb} and C_{cb}. The patch electrode is in contact with the cell body; the process of length L projects to the right. In cells with a complex morphology an elaborately branched dendritic tree is modeled as a single cylindrical process such as that shown here.

equivalent cylinder representation a popular model for cable analysis of neurons despite the fact that Rall's branching rules are usually not obeyed well by real dendrites.

Analysis of the Rall model is based on a modification of the equivalent circuit of Figure 6.6.4 to include a cylindrical process (Fig. 6.6.5). The mathematical solution to this problem predicts that the current response to a voltage step will be a sum of many exponentials (Rall and Segev, 1985). A single rapid exponential component of current is associated with the charging of the cell body, and a sum of several slower exponential components is associated with the charging of the process (Jackson, 1992). Fortunately, the rapid component of the current still has a time constant of $R_s C_{cb}$; however, C_{cb} is now the capacitance of the cell body rather than the whole cell. The fact that the rapid component of charging has this form allows one to determine R_s in the same manner as for cells with simple geometries. When using the transient cancellation circuitry on a cell with a complex shape, it is important to remember that during step 9 (see Basic Protocol 1) it is not possible to adjust the controls to remove the entire transient. No effort should be made to remove the slower components of the transient by overcompensating the fast component (Fig. 6.6.6). The slower process-charging components of current introduce an error in the determination of R_s and C_{cb}, which is related to the ratio of their summed amplitudes to the amplitude of the fast cell body–charging component. This error can be corrected as described elsewhere (Jackson, 1992).

In order to evaluate the space clamp problem, it is often helpful to think in terms of a quantity known as the length constant, λ, which has the form

$$\lambda = \sqrt{\frac{R_m d}{4 R_i}}$$

Equation 8

where R_m is the resistance of a unit area of membrane (typically ranging from 10,000 to >100,000 Ωcm^2), R_i is the cytoplasmic resistivity (typically 100 to 200 Ωcm), and d is the process diameter in centimeters (Rall, 1977). λ has units of length and gives the distance for an e-fold decay of voltage in an infinite cylindrical cable. If λ and the process length are known,

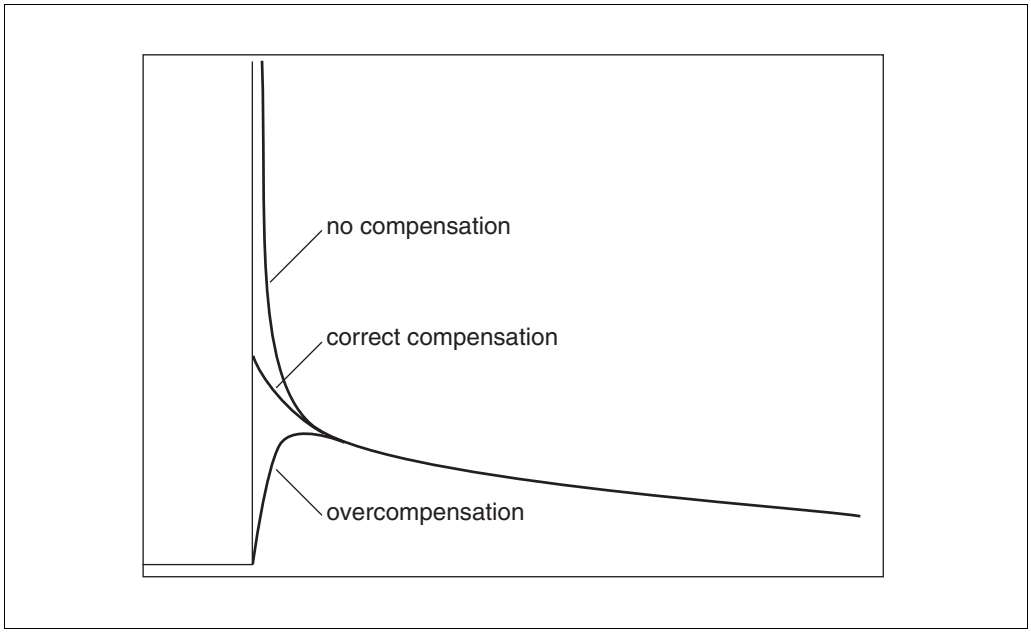

Figure 6.6.6 Examples of different degrees of compensation of the cell capacitance in a whole-cell voltage clamp recording from a cell with a process (as in Fig. 6.6.5). As in Figure 6.6.2E and F, the controls of the patch clamp amplifier are adjusted to remove the charging transient, but because the transient has several exponential components, complete cancellation cannot be achieved. With no compensation the large spike can be clearly seen. With overcompensation the current at the start of the pulse is brought back to zero in a misguided effort to compensate slower components of the transient.

the voltage along a process can be computed as a function of distance from the cell body. The function is an exponential only when the cable is infinite. For a cable of finite length, the function is a hyperbolic sine when the distal end is open,

$$V(X) = \frac{\sinh(L - X)}{\sinh(L)}$$

Equation 9

and a hyperbolic cosine when the distal end is sealed,

$$V(X) = \frac{\cosh(L - X)}{\cosh(L)}$$

Equation 10

where X is length in units of λ and L is the value of X at the end of the process (Rall, 1977).

The parameter L thus provides an important index for the effectiveness of space clamp. As explained in Basic Protocol 3 (cable analysis), L can be determined using current responses to small voltage steps and mathematical formulas based on cable theory (Rall, 1969, 1977; Rall and Segev, 1985; Jackson, 1992). One can also estimate L directly from morphological data, but this requires some idea of the value of λ. λ is shorter for narrower, finer processes, but is on the order of hundreds of microns even for very fine axons, so appreciable spatial variation in steady-state voltage requires fairly long processes.

A short electrotonic length (e.g., <0.3) might mean that a cell is electrically compact so that the voltage is more uniform. According to Equation 10, the voltage at the end will then be $V_{cb}/\cosh(0.3) = 0.96\ V_{cb}$, suggesting that the deviation from V_i will be only 4%. However, this calculation is valid only for a steady state in which voltage is not changing. The effective range over which voltage control is achieved will be more limited when the voltage is changing or channels are gating rapidly. Thus, even when channels are a short electrotonic distance from the patch electrode there can be a serious space-clamp problem. This has been well documented for synaptic potentials using simulation methods. Synaptic inputs to dendrites at electrotonic distances of only 0.1 can be subjected to substantial distortions (Johnston and Brown, 1983; Rall and Segev, 1985; Spruston et al., 1994).

Because the steady-state solutions (Equations 9 and 10) are inadequate with rapidly changing voltage and conductance, the time-

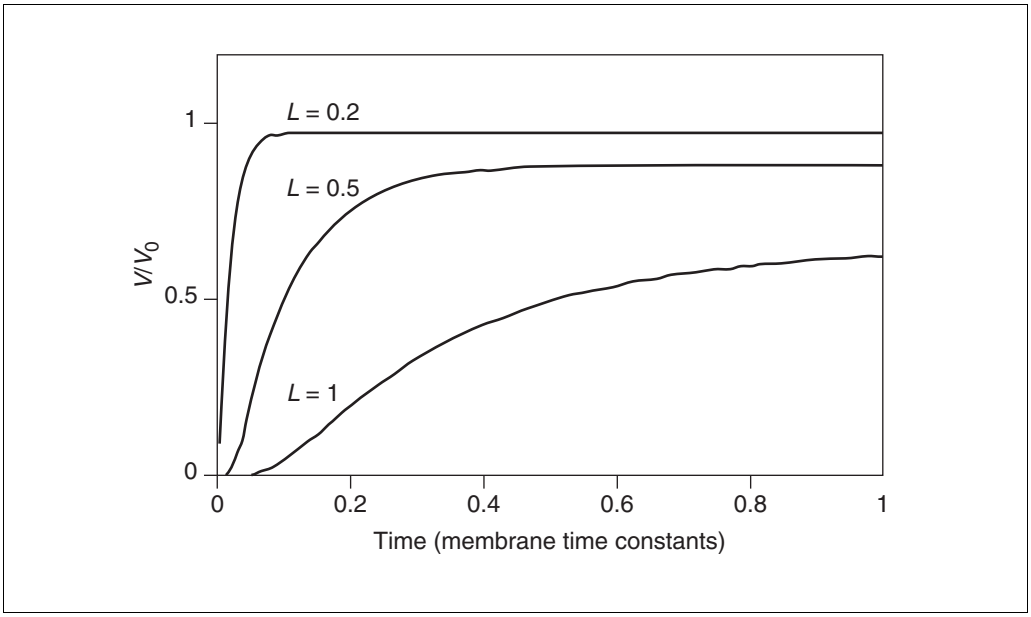

Figure 6.6.7 Plots of Equation 11 (truncated to 10 terms) show the settling of voltage at the end of a cylindrical process (such as that shown in Fig. 6.6.5) for a voltage pulse applied to the soma. The final voltage is the first term of Equation 11 (Equation 10), after the exponential decays are complete. The time axis is in units of the membrane time constant so even for $L = 0.2$, the settling time can be ~400 μsec (for a typical value of $\tau_m = 20$ msec). For the plots with longer L, the voltage at the end of the process can take several msec to settle to a steady state that differs significantly from V_c.

dependent solution of the cable equation should be considered. When point clamp is perfect, the response of a cable to a voltage step of amplitude V_0 is described by the following expression (Rall and Segev, 1985):

$$\frac{V(X,t)}{V_0} = \frac{\cosh(L-X)}{\cosh(L)} - \frac{2}{L}\sum_{n=1}^{\infty}\frac{\alpha_n \sin(\alpha_n X)}{1+\alpha_n^2}\, e^{-\left(1+\alpha_n^2\right)t/\tau_m}$$

Equation 11

where $\alpha_n = (2n-1)\pi/2L$. With knowledge of L and τ_m, estimated as described in Basic Protocol 3 (cable analysis), this expression can be plotted to see how the voltage will be expected to change at various electrotonic distances. The greatest space-clamp error will be at the end of the process, where $X = L$. Figure 6.6.7 shows the time course predicted by Equation 11 for voltage at the cable end ($X = L$) for processes of length $L = 0.2$, 0.5, and 1.0. This plot shows that even for a short process ($L = 0.2$), the voltage at the distal end requires ~0.02 membrane time constants to settle. For a typical value for τ_m of 20 msec, this would be 400 μsec. Equation 11 is easy to plot and can give some insight into what kinds of channel-gating processes can be resolved in cells with processes.

An alternative strategy for evaluating the dynamics of space clamp can be developed with the aid of the length constant for a sinusoidally varying command voltage. The length constant is then reduced according to the expression

$$\lambda(f) = \frac{\lambda_0}{\sqrt{\frac{1+\sqrt{1+(\tau_m f/2\pi)^2}}{2}}}$$

Equation 12

where λ_0 is the zero-frequency length constant from Equation 8 and f is the frequency for a sinusoidal voltage input signal (Traub and Miles, 1991). This equation shows that high-frequency signals spread less effectively than low-frequency signals. Because the dynamic response of a voltage clamp to a conductance change is similar to the dynamic response of a voltage clamp to voltage change (Finkel and Gage, 1985), we might expect Equation 12 to provide a length constant relevant to a voltage clamp's ability to follow conductance changes occurring in a dendrite. If we use the time constant for a given channel-gating process to replace $2\pi/f$ in Equation 12, we can obtain a rough estimate of the extent of voltage control

specifically relevant to that process. Because τ_m is typically >20 msec and we are often interested in channel-gating processes with time constants of 1 msec, we can approximate and simplify Equation 12 to give

$$\lambda(\tau) \approx \lambda_0 \sqrt{\frac{2\tau}{\tau_m}}$$

Equation 13

For a gating process with a time constant ten times faster than the membrane time constant, the length constant will decrease by a factor of 2.3 so that an apparent L will be that much greater than an estimate based on steady-state theory. When a gating process is fifty times faster than τ_m the electrotonic length will be five times greater. Thus, channels 0.1 length constant away will behave as though they are 0.5 length constants away for a channel-gating process of this speed. For a process with L = 0.3 in the steady state, L becomes 1.5 for fast conductance changes, and the voltage at the end of the process becomes 0.42 V_{cb} (from Equation 10) instead of 0.96 V_{cb} as mentioned above. This large error illustrates that cells are far less compact than the steady-state expressions would suggest when voltage or membrane conductance change rapidly.

As another way to evaluate the space-clamp error, L and τ_m can be measured in cells (see Basic Protocol 3, cable analysis). Equation 12 or Equation 13 can then be used to obtain the factor by which the length constant will be reduced for a kinetic process with a known time constant. L can then be multiplied by this factor to obtain a value L' that is relevant to the kinetic process under study. The voltage error at the end of the process can then be estimated for a sealed cable (Equation 10) as 1/cosh(L').

These methods of evaluating space clamp are based on the validity of the equivalent cylinder representation for the processes of the cell under study. It is important to test this hypothesis in each case, and cable analysis provides some methods for doing so. Note that L in Equation 2 cannot be computed for $\tau_1/\tau_2 >$ 9. If this happens, the transient has no equivalent cylinder representation. However, the converse is not true; $\tau_1/\tau_2 < 9$ does not prove that the process has a valid equivalent cylinder representation. Other more stringent criteria can be used to test this hypothesis (Jackson, 1992). If the tests are not satisfied, the process may not have a simple equivalent geometry, and cable analysis could then be very difficult. Additional practical guides and application examples for cable analysis with the whole-cell voltage clamp can be found in Jackson (1992), with applications of cable theory to more complicated branching structures in Major et al. (1993) and applications to an axon with a distal swelling in Jackson (1993).

Anticipated Results

Current-voltage plots

When interpreting current-voltage (I-V) plots obtained from voltage-clamp data one assumes that for a given type of channel the total current is equal to the number of channels, N, times the average current per channel. The average current per channel in turn is equal to the single-channel current, i, times the probability that a channel is open, P_o. To a first approximation an open channel behaves like a simple linear resistor with a reversal potential that depends on the ion selectivity of the channel. This gives $i = g(V - V_r)$ where g is the single-channel conductance and V_r is the reversal potential. Total current is then

$$I = NP_o g(V - V_r)$$

Equation 14

When all the channels are open, P_o = 1 and the conductance is maximum. We can thus consolidate two variables into the maximum conductance as $G_{max} = Ng$ to obtain

$$I = P_o G_{max}(V - V_r)$$

Equation 15

In general, P_o increases smoothly from zero to one as voltage is varied, while the rest of the expression for current, $G_{max}(V - V_r)$, is simply a line with slope G_{max} and intercept V_r. By allowing P_o to increase over various voltage ranges relative to V_r, a variety of I-V plots can be generated. If P_o increases as one moves toward V_r from the left (i.e., negative to V_r), the current will become increasingly negative even as the driving force for the ion in question decreases. This gives the I-V plot a negative slope. On the other hand, when P_o increases as one moves away from V_r to the right (positive to V_r), a nearly flat line starts to curve upward to reach a limiting slope of NG_{max}. In this way a rich variety of behaviors can be obtained. For further discussion of I-V plots and voltage dependent channels see Hille (1992).

The Boltzmann equation

Interpretation of voltage clamp data often entails fitting the voltage dependence of the state of a channel (P_o in discussion of I-V plots) to a physical model for voltage gating, and the starting point for such models is the Boltzmann equation. Representing channel gating as a transition between an open state and a closed state, we have

$$C \underset{\beta}{\overset{\alpha}{\rightleftharpoons}} O$$

Equation 16

where α is the opening rate, β is the closing rate, and the equilibrium constant between the two conformations is α/β. At equilibrium, the ratio of the number of channels in the open state to the number of channels in the closed state is obtained from the free energy difference, ΔG, as

$$N_o / N_c = e^{-\Delta G/RT}$$

Equation 17

where R is the gas constant and T is the temperature. If during the transition between the open and closed states a charged group that is part of the protein moves within the electric field across the membrane, then the movement of this charge will make a contribution to ΔG equal to $z F \delta V$, where z is the valence of the charge, F is Faraday's constant, and δ is the fraction of the transmembrane potential traversed as the charge moves during the interconversion. This allows ΔG to be separated into voltage-independent and voltage-dependent terms

$$\Delta G = \Delta G_o + V F \sum_i \delta_i z_i$$

Equation 18

where the second term on the right represents the summed contributions to the voltage dependence of many charges moving through different fractions of the membrane potential during gating. Substituting Equation 18 into Equation 17, and then rearranging to obtain the fraction of channels in the open state, we obtain

$$P_o = \frac{N_o}{N_o + N_c} = \frac{1}{1 + e^{\frac{\Delta G_o + V F \Sigma \delta_i z_i}{RT}}}$$

Equation 19

This is the Boltzmann equation. It shows how the probability of being open varies from 0 to 1 as voltage is changed. It is more commonly used in the form

$$P_o = \frac{1}{1 + e^{(V - V_o)/\kappa}}$$

Equation 20

where $-V_o/\kappa$ replaces $\Delta G_o/RT$ and $1/\kappa$ replaces $F\Sigma \delta_i z_i/RT$. Equation 20 can be used in place of P_o. For analyzing real conductance data one often uses a more general expression:

$$G = G_{min} + \frac{G_{max} - G_{min}}{1 + e^{(V - V_o)/\kappa}}$$

Equation 21

where G_{min} is the minimum conductance. This equation is plotted in Figure 6.6.8 to illustrate the significance of the various parameters. G_{min} reflects the presence of a voltage-independent channel-gating transition or membrane leak. V_o and κ are generally considered to be important characteristics of a voltage-gated channel that reflect its molecular properties. Equation 21 can be fitted to voltage-clamp data by varying the parameters V_o and κ (and possibly G_{min} and G_{max}, as well). V_o is the midpoint of the transition, or the voltage when half of the channels are open (Fig. 6.6.8). κ is called the "steepness" or "slope" factor, and provides a rough index of how much charge moves during the gating transition. See Hille (1992) for further discussion of the relevance of the Boltzmann equation to voltage-dependent channel gating. For an excellent example of the application of these concepts to a K^+ channel, see Schoppa et al. (1992).

Exponential relaxations in channels

Channel gating often follows exponential kinetics. With the two-state gating scheme as in the preceeding section, we can obtain a differential equation for the change in the number of open channels with time

$$\frac{dN_o}{dt} = \alpha N_c - \beta N_o$$

Equation 22

Solving this equation and converting channel number to current (Equation 11) gives

$$I = (I_i - I_f)\left(1 - e^{t/\tau}\right) + I_f$$

Equation 23

Fitting this expression to current versus time then gives the time constant, $\tau = 1/(\alpha + \beta)$. The initial and final currents, I_i and I_f, reflect the equilibrium open probabilities in Equation 20 for the voltage before and after the step, respec-

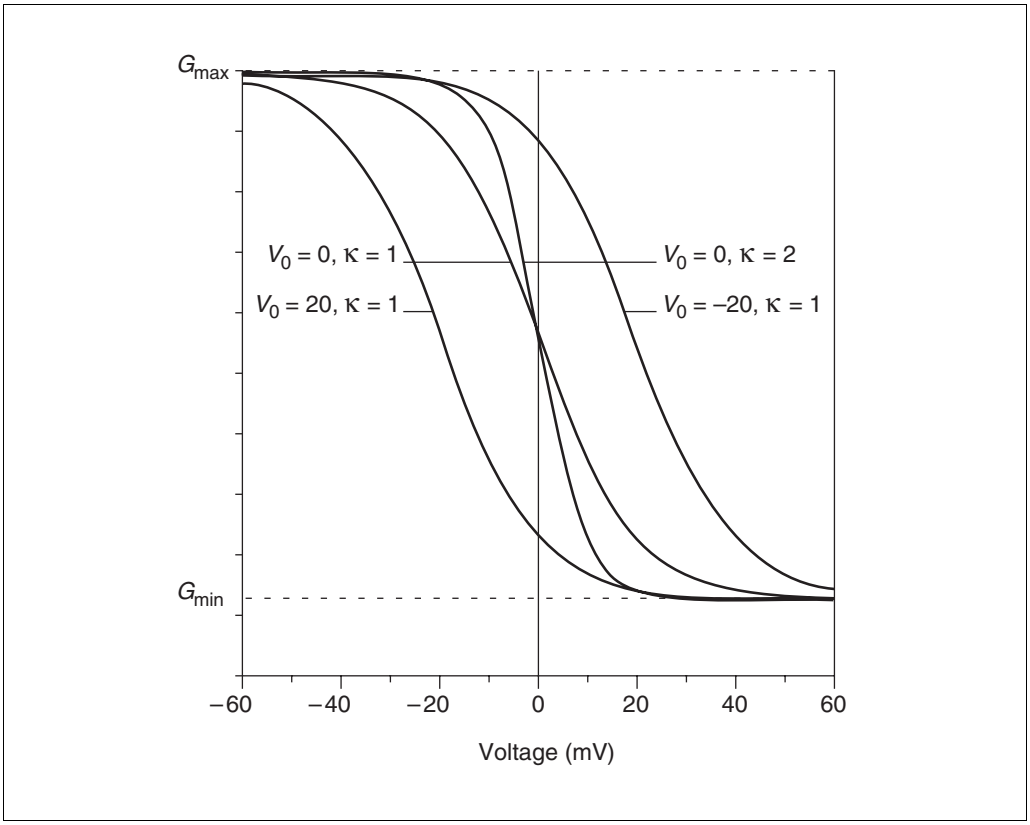

Figure 6.6.8 Plots of the Boltzmann equation (Equation 21) illustrate how the probability of channel opening can change with voltage. The parameter V_0 influences the voltage midpoint as shown. The parameter κ influences the steepness. The conductance varies from G_{min} to G_{max}.

tively. More complex gating schemes can be developed by incorporating additional closed and open states into a model. Such models can be shown to exhibit multiexponential kinetics (Colquhoun and Hawkes, 1977).

A particularly important extension of the two-state gating scheme arises from combining a small number of independent voltage sensing elements (protein subunits), and coupling them to one channel. If channel opening is assumed to require the gating of all of the subunits, then the probability of channel opening will be the probability of a single subunit having undergone the voltage-gated transition, raised to the power of the number of subunits. For n subunits, it is easy to see that Equation 23 then becomes

$$I = (I_i - I_f)\left(1 - e^{t/\tau}\right)^n + I_f$$

Equation 24

Such expressions were used to model current activation kinetics in the squid axon by Hodgkin and Huxley (1952b), who found n = 3 for Na^+ current and n = 4 for K^+ current.

Time Considerations

Electrode fabrication will require ~10 min (see *UNIT 6.3*) prior to beginning the recording. Positioning the electrode and running test currents requires ~1 min. Forming an adequate gigaseal can take up to several minutes, as can breaking into the cell. Recording capacitance and adjusting R_s compensation take <1 min. Time required for data acquisition from one cell varies from ~5 min to 1 to 2 hr. Time required for data analysis can be as little as 1 hr, but if many traces have been collected and analysis involves fitting to complex models, considerably more time will be needed.

Literature Cited

Adams, M.E. and Swanson, G. 1996. Neurotoxins, 2nd ed. Supplement to *Trends in Neuroscience*.

Armstrong, C.M. and Gilly, W.F. 1992. Access resistance and space clamp problems associated with whole-cell patch clamping. *Methods Enzymol.* 207:100-122.

Banks, M.I., Haberly, L.B., and Jackson, M.B. 1996. Layer-specific properties of the transient K-current (I_a) in piriform cortex. *J. Neurosci.* 16:3862-3876.

Bean, B.P. 1992. Whole-cell recording of calcium channel currents. *Methods Enzymol.* 207:181-193.

Bielefeldt, K., Rotter, J.L., and Jackson, M.B. 1992. Three potassium channels in rat posterior pituitary nerve endings. *J. Physiol.* 458:41-67.

Carbone, E. and Lux, H.D. 1986. Sodium channels in cultured dorsal root ganglion neurons. *Eur. J. Biophys.* 13:259-271.

Carbone, E. and Lux, H.D. 1987. Kinetics and selectivity of a low-voltage-activated calcium current in chick and rat sensory neurones. *J. Physiol.* 386:547-570.

Cole, K.S. 1949. Dynamic electrical characteristics of the squid axon membrane. *Arch. Sci. Physiol.* 3:253-258.

Colquhoun, D. and Hawkes, A.G. 1977. Relaxation and fluctuation of membrane currents that flow through drug operated ion channels. *Proc. R. Soc. Lond. B Biol. Sci.* 199:231-262.

Cota, G. 1986. Calcium currents in pars intermedia cells of the rat pituitary gland. *J. Gen. Physiol.* 88:83-105.

Cota, G. and Armstrong, C.M. 1988. Potassium channel "inactivation" induced by soft-glass patch pipettes. *Biophys. J.* 53:107-109.

Cota, G. and Armstrong, C.M. 1992. Analysis of sodium channel tail currents. *Methods Enzymol.* 207:806-816.

De Schutter, E. 1989. Computer software for development and simulation of compartmental models of neurons. *Comput. Biol. Med.* 19:71-81.

Fenwick, E.M., Marty, A., and Neher, E. 1982. Sodium and calcium channels in bovine chromaffin cells. *J. Physiol.* 331:599-636.

Finkel, A.S. and Gage, P.W. 1985. Conventional voltage clamping with two intracellular microelectrodes. *In* Voltage and Patch Clamping with Microelectrodes (T.G. Smith, H. Lecar, S.J. Redman, and P.W. Gage, eds.) pp. 47-94. American Physiological Society, Bethesda.

Forscher, P. and Oxford, G.S. 1985. Modulation of calcium channels by norepinephrine in internally perfused dialyzed avian sensory neurons. *J. Gen. Physiol.* 85:743-763.

Fox, A.P., Nowycky, M.C., and Tsien, R.W. 1987. Kinetic and pharmacologic properties distinguishing three types of calcium currents in chick sensory neurones. *J. Physiol.* 394:149-172.

Hamill, O.P., Marty, A., Neher, E., Sakmann, B., and Sigworth, F.J. 1981. Improved patch clamp techniques for high-resolution current recording from cells and cell-free membrane patches. *Pfluegers Arch. Eur. J. Physiol.* 391:85-100.

Heinemann, S.H. 1995. Guide to data acquisition and analysis. *In* Single-Channel Recording (B. Sakmann and E. Neher, eds.) pp. 53-91. Plenum, New York.

Herrington, J. and Bookman, R.J. 1994. Pulse Control V4.3: Igor XOPS for Patch Clamp Data Acquisition. University of Miami Press, Miami.

Hille, B. 1992. Ion Channels of Excitable Membranes. Sinauer Associates, Sunderland, Mass.

Hodgkin, A.L. and Huxley, A.F. 1952a. Currents carried by sodium and potassium ions through the membrane of the giant axon of *Loligo*. *J. Physiol.* 116:449-472.

Hodgkin, A.L. and Huxley, A.F. 1952b. A quantitative description of membrane current and its application to conduction and excitation in nerve. *J. Physiol.* 117:500-544.

Hoshi, T., Rothlein, J., and Smith, S.J. 1984. Facilitation of Ca^{2+}-channel currents in bovine adrenal chromaffin cells. *Proc. Natl. Acad. Sci. U.S.A.* 81:5871-5875.

Howe, J.R. and Ritchie, J.M. 1992. Multiple kinetic components of sodium channel inactivation in rabbit Schwann cells. *J. Physiol.* 455:529-66.

Huguenard, J.R. and Prince, D.A. 1992. A novel T-type current underlies prolonged Ca^{2+}-dependent burst firing in GABAergic neurons of rat thalamic reticular nucleus. *J. Neurosci.* 12:3804-3817.

Jackson, M.B. 1992. Cable analysis with the whole-cell patch clamp: Theory and experiment. *Biophys. J.* 61:756-766.

Jackson, M.B. 1993. Passive current flow and morphology in the nerve terminal arborizations of the posterior pituitary. *J. Neurophysiol.* 69:692-702.

Jackson, M.B. and Zhang, S.J. 1995. Action potential propagation and propagation block by GABA in rat posterior pituitary nerve terminals. *J. Physiol.* 483:597-611.

Johnston, D. and Brown, T.H. 1983. Interpretation of voltage clamp measurements in hippocampal neurons. *J. Neurophysiol.* 50:464-486.

Jones, S.W. 1987. Sodium currents in dissociated bull-frog sympathetic neurones. *J. Physiol.* 389:605-627.

Jones, S.W. 1990. Whole-cell and microelectrode voltage clamp. *In* Neuromethods, Vol. 14 (A.A. Boulton, G.B. Baker, and C.H. Vanderwolf, eds.) pp. 143-192. Humana Press, Totowa, NJ.

Jones, S.W. and Marks, T.N. 1989. Calcium currents in bullfrog sympathetic neurons. I. Activation kinetics and pharmacology. *J. Gen. Physiol.* 94:151-167.

Kay, A.R. and Wong, R.K.S. 1987. Calcium current activation kinetics in isolated pyramidal neurones of the CA1 region of the mature guinea-pig hippocampus. *J. Physiol.* 392:603-616.

Kostyuk, P.G. 1988. Cytoplasmic modulation of ion channel functioning in the neuronal membrane. *In* Calcium and Ion Channel Modulation (A.D. Grinnell, D. Armstrong, and M.B. Jackson, eds.) pp. 187-195. Plenum, New York.

Major, G., Evan, J.D., and Jack, J.B. 1993. Solutions for transients in arbitrarily branching cables: I. Voltage recording with a somatic shunt. *Biophys. J.* 65:423-449.

Malécot, C.O., Feindt, P., and Trautwein, W. 1988. Intracellular N-methyl-D-glucamine modifies the kinetics of calcium current in guinea pig ventricular heart cells. *Pfluegers Arch. Eur. J. Physiol.* 411:235-242.

Marmont, G. 1949. Studies on the axon membrane: A new method. *J. Cell. Comp. Physiol.* 34:351-382.

Marty, A. and Neher, E. 1985. Potassium channels in cultured bovine adrenal chromaffin cells. *J. Physiol.* 367:117-141.

Marty, A. and Neher, E. 1995. Tight-seal whole-cell recording. *In* Single-Channel Recording (B. Sakmann and E. Neher, eds.) pp. 31-51. Plenum, New York.

Monyer, H. and Jonas, P. 1995. Polymerase chain reaction analysis of ion channel expression in single neurons of brain slices. *In* Single-Channel Recording (B. Sakmann and E. Neher, eds.) pp. 357-373. Plenum, New York.

Neher, E. 1992. Correcting for liquid junction potentials in patch clamp experiments. *Methods Enzymol.* 207:123-131.

Numann, R.E., Wadman, W.J., and Wong, R.K. 1987. Outward currents of single hippocampal cells obtained from the adult guinea-pig. *J. Physiol.* 393:331-353.

Oxford, G.S. 1981. Some kinetic and steady-state properties of sodium channels after removal of inactivation. *J. Gen. Physiol.* 77:1-22.

Oxford, G.S. and Wagoner, P.K. 1989. The inactivating K^+ current in GH_3 pituitary cells and its modification by chemical reagents. *J. Physiol.* 410:587-612.

Pusch, M. and Neher, E. 1988. Rates of diffusional exchange between small cells and a measuring patch pipette. *Pfluegers Arch Eur. J. Physiol.* 411:204-211.

Rall, W. 1959. Branching dendritic trees and motoneuron membrane resistivity. *Exp. Neurol.* 1:491-527.

Rall, W. 1969. Time constants and electrotonic length of membrane cylinders and neurons. *Biophys. J.* 9:1483-1508.

Rall, W. 1977. Core conductor theory and cable properties of neurons. *In* Handbook of Physiology. The Nervous System. Cellular Biology of Neurons (J.M. Brookhart and V.B. Mountcastle, eds.) pp. 39-97. American Physiological Society, Bethesda.

Rall, W. and Segev, I. 1985. Space clamp problems when voltage clamping branched neurons with intracellular microelectrodes. *In* Voltage and Patch Clamping with Microelectrodes (T.G. Smith, H. Lecar, S.J. Redman, and P.W. Gage) pp. 191-215. American Physiological Society, Bethesda.

Sakmann, B. and Neher, E. 1995a. Geometric parameters of pipettes and membrane patches. *In* Single-Channel Recording (B. Sakmann and E. Neher, eds.) pp. 637-650. Plenum, New York.

Sakmann, B. and Neher, E. 1995b. Single-Channel Recording. Plenum, New York.

Schoppa, N.E., McCormack, K., Tanouye, M.A., and Sigworth, F.J. 1992. The size of gating charge in wild type and mutant *Shaker* potassium channels. *Science* 255:1712-1715.

Sigworth, F.J. 1995. Electronic design of the patch clamp. *In* Single-Channel Recording (B. Sakmann and E. Neher, eds.) pp. 95-127. Plenum, New York.

Smith, T.G., Lecar, H., Redman, S.J., and Gage, P.W. (eds). 1985. Voltage and Patch Clamping with Microelectrodes. American Physiological Society, Bethesda.

Spruston, N., Jaffe, D.B., and Johnston, D. 1994. Dendritic attenuation of synaptic potentials and currents: The role of passive membrane properties. *Trends Neurosci.* 17:161-166.

Swandulla, D. and Armstrong, C.M. 1988. Fast-deactivating calcium channels in chick sensory neurons. *J. Gen. Physiol.* 92:197-218.

Swandulla, D. and Chow, R.H. 1992. Recording solutions for isolating specific ionic channel currents. *In* Practical Electrophysiological Methods (H. Kettenmann and R. Grantyn, eds.) pp. 164-168. Wiley-Liss, New York.

Traub, R.D. and Miles, R. 1991. Neuronal Networks of the Hippocampus. Cambridge University Press, New York.

Yamaguchi, K., Nakajima, Y., Nakajima, S., and Stanfield, P.R. 1990. Modulation of inwardly rectifying channels by substance P in cholinergic neurones from rat brain in culture. *J. Physiol.* 426:499-520.

Zagotta, W.N. and Aldrich, R.W. 1990. Voltage-dependent gating of Shaker A-type potassium channels in *Drosophila* muscle. *J. Gen. Physiol.* 95:29-60.

Zhang, H.G., ffrench-Constant, R.H., and Jackson, M.B. 1994. A unique amino acid of the *Drosophila* GABA receptor influences drug sensitivity by two mechanisms. *J. Physiol.* 479:65-75.

Internet Resources

http://chroma.med.miami.edu/cap

Site to download Pulse Control (see Strategic Planning, section on Computer, interface, and software).

Contributed by Meyer B. Jackson
University of Wisconsin Medical School
Madison, Wisconsin